Alma Mater Studiorum – Università di Bologna

DOTTORATO DI RICERCA IN
CHIMICA

Ciclo XXVII

Settore Concorsuale di afferenza: 03/A1
Settore Scientifico disciplinare: CHIM 01

New analytical LC-mass spectrometry methodologies for the quali-quantitative determination of natural substances and drugs in complex matrices

Presentata da: Silvia Spinozzi

Coordinatore Dottorato
Prof. Aldo Roda

Relatore
Prof. Aldo Roda

Esame finale anno 2015

Content

Prefazione

Abstract

Prefazione

“Abbiamo spesso sentito sostenere la tesi che le scienze sono fondate su concetti basilari chiari e nettamente definiti. In verità nessuna scienza, neanche la più esatta, inizia con tali definizioni. Il vero inizio dell’attività scientifica consiste piuttosto nel descrivere i fenomeni e quindi nel raggrupparli, classificarli e correlarli. Già allo stadio di descrizione non è possibile evitare di applicare certe idee astratte al materiale in questione, che derivano da qualche parte, ma che certamente sono basate unicamente sulle nuove osservazioni. Tali idee –che in seguito diventeranno I concetti basilari della scienza- sono ancora più indispensabili quando il materiale viene ulteriormente elaborato. Dapprima esse devono necessariamente possedere un certo grado di indefinitezza; non si può neanche considerare una chiara delimitazione del loro contenuto. Finché queste idee rimangono in questo stato, noi arriviamo a capirne il significato facendo spesso riferimento al materiale di osservazione da cui sembra scaturire, ma al quale, in realtà, sono state imposte. Così a rigor di termini, esse non sono che convenzioni, benché tutto dipenda dal fatto che non sono scelte arbitrariamente, ma determinate in dipendenza dai loro rapporti che noi intuiamo anche prima di poterli riconoscere e dimostrare. Siamo in grado di formulare i basilari concetti scientifici con maggior precisione solo dopo un’indagine più profonda del campo di osservazione, e progressivamente possiamo modificarli sicché diventino utili e coerenti quando vengono applicati a un’area più estesa. A quel punto è arrivato il momento di regalarli alla scienza. Il progresso della scienza, comunque, non tollera alcuna rigidità nemmeno nelle definizioni. La fisica e la chimica forniscono degli eccellenti esempi di definizioni che vanno sempre alterati nel loro contenuto.”

Sigmund Freud- Metapsicologia

Abstract

This thesis reports an integrated analytical and physicochemical approach for the study of natural substances and new drugs based on mass spectrometry techniques combined with liquid chromatography.

In particular, Chapter 1 concerns the study of Berberine a natural substance with pharmacological activity for the treatment of hepatobiliary and intestinal diseases. The first part focused on the relationships between physicochemical properties, pharmacokinetics and metabolism of Berberine and its metabolites. For this purpose a sensitive HPLC-ES-MS/MS method have been developed, validated and used to determine these compounds during their physicochemical properties studies and plasma levels of berberine and its metabolites including berberrubine(M1), demethylenberberine(M3), and jatrorrhizine(M4) in humans. Data show that M1, could have an efficient intestinal absorption by passive diffusion due to a keto-enol tautomerism confirmed by NMR studies and its higher plasma concentration. In the second part of Chapter 1, a comparison between M1 and BBR in vivo biodistribution in rat has been studied.

In Chapter 2 a new HPLC-ES-MS/MS method for the simultaneous determination and quantification of glucosinolates, as glucoraphanin, glucoerucin and sinigrin, and isothiocyanates, as sulforaphane and erucin, has developed and validated. This method has been used for the analysis of functional foods enriched with vegetable extracts.

Chapter 3 focused on a physicochemical study of the interaction between the bile acid sequestrants used in the treatment of hypercholesterolemia including colesevelam and cholestyramine with obeticolic acid (OCA), potent agonist of nuclear receptor farnesoid X (FXR). In particular, a new experimental model for the determination of equilibrium binding isotherm was developed.

Chapter 4 focused on methodological aspects of new hard ionization coupled with liquid chromatography (Direct-EI-UHPLC-MS) not yet commercially available and potentially useful for qualitative analysis and for “transparent” molecules to soft ionization techniques. This method was applied to the analysis of several steroid derivatives.

Chapter 1

Nutraceutical: berberine and its metabolites

In recent years, there is a growing interest in "nutraceuticals" which provide health benefits and are alternative or complementary to the use of conventional drugs in modern medicine. The term “nutraceutical” was coined from “nutrition” and “pharmaceutical”. According to DeFelice definition, nutraceutical can be defined “as a food (or part of a food) that provides medical or health benefits, including the prevention and/or treatment of several diseases”[1].

In this definition, nutrients, herbals and dietary supplements, that contain one or more bioactive molecules, are included. Most commercially nutraceuticals contain a single purified natural substance perpetrated from raw extracts in different foods products. The active ingredient often exceeds the amount present in the whole plant. Indeed, the rationale used in nutraceutical field is that the administered doses of these supplements should be as high as in conventional drugs. In this way, a nutraceutical and a drug could have the same therapeutic effect. Nevertheless unlike drugs, nutraceuticals do not require conventional approval based on a detailed characterization (toxicological studies, metabolism) of its constituents, undermining the consumers’ safety. Indeed, often the non- declared compounds are present in these supplements even at higher amount than the declared bioactive molecule. To make matters worse, their physicochemical properties, biodistribution in the human body and target organ activity have been poorly studied despite nutraceuticals administration at high doses (from 0.5 to 2g/day). The row material and natural extract could be purchased by uncontrolled suppliers and this is an additional concern for the consumer’s safety.

1.1 Berberine

1.1.1 Pharmacological and therapeutic effects

Berberis vulgaris L. extracts have been used for a long time in traditional Indian and Chinese medicine used as antimicrobial against a variety of organisms such as bacteria, viruses, fungi, protozoans, helminthes, and chlamydia[2]. Studies carried out on the chemical composition of these extracts show that the major isoquinoline alkaloid constituents were berberine and palmitine. Recently, Berberine (BBR, **Figure 1**) has intrigued increasing interest in its several bioactivities as antifungal[3], anti-inflammatory[4], antimalarial[5], anti-HIV[6], antihyperglycemic[7], immunoregulatory[8], antitumor[9].

Clinical trials showed also the beneficial effects of berberine in hypercholesterolemic patients and type 2 diabetes[10]. Indeed, administration of Berberine 500mg/die decreased the levels of total cholesterol, LDL-cholesterol and triglycerides (*i.e.* about 29, 25 and 35%). In particular, BBR increase low-density-lipoprotein receptor (LDLR) expression by stabilization of LDLR mRNA by activation of extracellular signal-regulated kinase (ERK). In addition, BBR was active in enhancing the expression of insulin receptor (InsR).

1.1.2 Metabolism of berberine

Previous studies[11] showed that BBR is metabolized in the liver by CYP450 isoenzymes through oxidative demethylation at positions 2, 3, 9, and 10 followed by conjugation of these hydroxyl group functions with glucuronic acid. In humans, the main primary metabolites of BBR

Figure 1) report the chemical structure of the main metabolites berberrubine (M1), thalifendine (M2), demethyleneberberine (M3), and jatrorrhizine (M4).

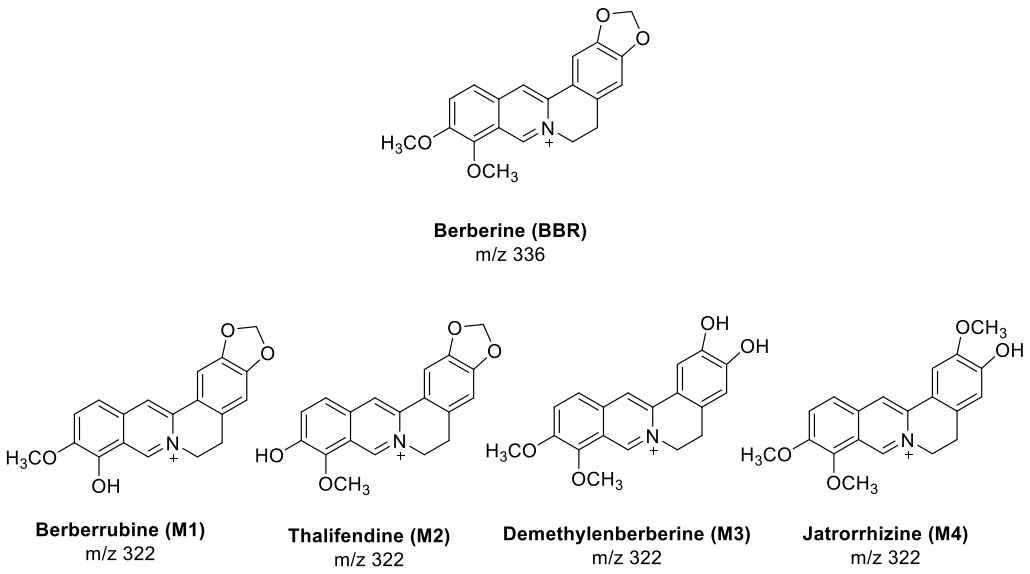

Figure 1. Primary hepatic metabolism of BBR

As well as BBR, its metabolites exhibit some pharmacological properties such as up-regulation of low-density lipoprotein receptor, and mRNA expression[12]. Among these, M1 showed the best up-regulatory effect for LDLR mRNA expression, although its activity was lower than BBR (**Figure 2**). Toxicity studies of metabolites have not yet been carried out as well as have not been evaluated their possible side effects.

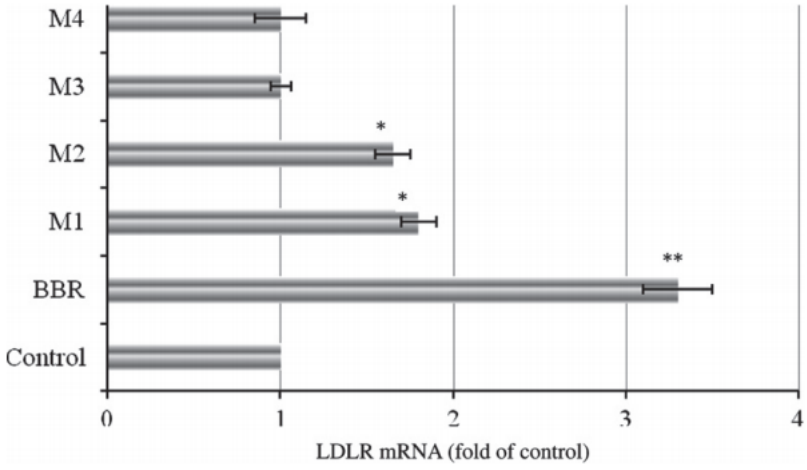

Figure 2. Effect of BBR and its metabolites on LDLR gene expression

1.1.3 Aim and rationale

Protoberberine (5,6-dihydrodibenzo[a,g]quinolizinium), alkaloids found in the bark, rhizomes, roots, and stems of Berberis vulgaris L. (Berberidaceae)[2], show many different types of biological activities. Among them, berberine (BBR, **Figure 1**) is the most interesting compound, which has a multi-target activity in particular as cholesterol-lowering effect[10].

In the last 20 years the study of natural substances has changed radically, but nowadays is still lacking a complete physicochemical characterization of biologically active natural molecules and even more of its major metabolites in vivo. This fact represents a bottleneck in lead discovery for pharmaceutical research based on natural sources. Indeed, the importance of physicochemical properties of molecules in the development of orally bioavailable drugs has been recognized. Even though nutraceuticals do not require a conventional drug approval for which pharmacokinetic, metabolism and safety studies must be conducted.

For this reasons, the aim of this study is to develop and validate a new HPLC-ES-MS/MS method for the qualitative and quantitative determination of BBR and its metabolites. This method will be used to accurately quantify BBR and its metabolites during studies regarding the measurements of their physicochemical properties, including lipophilicity, solubility, pKa, and albumin binding.

In addition, to better understand BBR and its metabolites pharmacokinetic, intestinal absorption and biodistribution in target organs, the plasma levels of BBR and its metabolites after acute and chronic oral administration to hypercolesterolemic patients will be investigated. The biomarker of hypercholesterolemia activity (total, LDL and HDL cholesterol, total triglycerides) will be monitored in hypercolesterolemic patients chronically treated with BBR.

Finally, the relationship between the plasma levels and physicochemical properties of BBR and its metabolites will be critically discussed.

1.1.4 Experimental

1.1.4.1 Materials and reagents

Berberine chloride (BBR-Cl) and jatrorrhizine chloride (M4-Cl), as a standard for HPLC (purity ≥97%), were purchased from Sigma (St. Louis, MO, USA) and AlloraChem srl (Rimini, Italy) respectively.

Berberrubine and demethylberberine were synthetized in Prof. M. Roberti Laboratory (Department of Pharmacy and Biotechnology, University of Bologna). Flash column chromatography was performed on silica gel (particle size 40−63 μm, Merck). (R,S)-noscapine, used as internal standard and Tris-HCl salt were purchased from Sigma (St. Louis, MO, USA).

The organic solvents used have HPLC-grade: methanol and acetonitrile were purchased from Carlo Erba Reagents (Milan, Italy) and LiChrosolv. HPLC-grade water was prepared using the Millipore Milli-Q Synthesis A10 system (Molsheim, France).

Berberis Vulgaris 250 mg capsules were purchased from KOS s.r.l. (Comeana, Italy). Oasis HLB (hydrophilic–lipophilic balance 200 mg, 6 mL) SPE columns were purchased from Waters (Milan, Italy)

1.1.4.2 Synthesis of berberine metabolites

Berberrubine

Berberrubine chloride was prepared starting from berberine chloride following two different procedures, reported in **Figure 3**. In particular, in the first procedure (a) berberrubine chloride was obtained by berberine chloride pyrolysis, heated at 195°-200° C for 10-15 min, in solvent-free conditions under vacuum[13] (20-30 mmHg), washed with ethanol and filtered (yield 81%).

^{1}H-NMR (DMSO-d_6, 400 MHz): δ 3.10 (t, 2H, J= 6.0 Hz), 3.79 (s, 3H), 4.54 (t, 2H, J= 6.0 Hz), 6.16 (s, 2H), 6.41 (d, 1H, J= 8 Hz), 7.02 (s, 1H), 7.27 (d, 1H, J= 8 Hz), 7.67 (s, 1H),

8.04 (s, 1H), 9.14 (s, 1H). 13C-NMR (DMSO-d6, 100 MHz): δ 27.5, 52.3, 55.7, 100.6, 101.5, 104.7, 108.2, 117.1, 120.0, 121.2, 121.8, 129.2, 132.0, 133.2, 145.7, 147.3, 148.3, 149.7, 167.3; MS (ES): m/z 322 ($M+H^+$).

In procedure b, berberine chloride was irradiate at 250 W, 200°C for 10-15 min, washed with ethanol and filtered (yield 62%)[14].

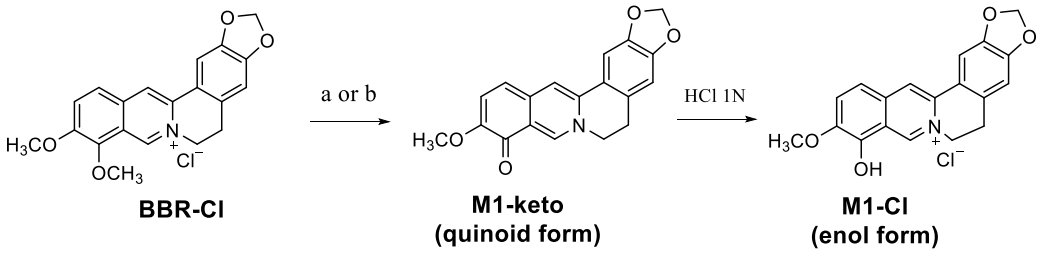

(a) BBR-Cl, 190-200° C, 30-40 mmHg, 15-20 min; **(b) BBR-Cl**, MW, 250 W, 200°C, 10-15 min

Figure 3. Synthesis of berberubine (M1)

^{1}H-NMR (DMSO-d_6, 400 MHz): δ 3.25 (t, 2H, J= 6 Hz), 4.10 (s, 3H), 4.96 (t, 2H, J= 6 Hz), 6.23 (s, 2H), 7.12 (s, 1H), 7.76 (d, 1H, J= 8 Hz), 7.84 (s, 1H), 8.15 (d, 1H, J= 8 Hz), 8.89 (s, 1H), 9.97 (s, 1H), 11.32 (br s, 1H). 13C-NMR (DMSO-d6, 100 MHz): δ 26.5, 54.9, 57.1, 102.0, 105.4, 108.4, 117.6, 118.1, 119.8, 120.7, 125.5, 130.5, 132.4, 136.6, 143.7, 145.4, 145.8, 147.7, 149.6.

Demethylenberberine

The semi-synthesis of demethylenberberine through the hydrolysis reaction of the berberine chloride acetal ring, in the presence of sulfuric acid and phloroglucin, was reported in

Figure 4.

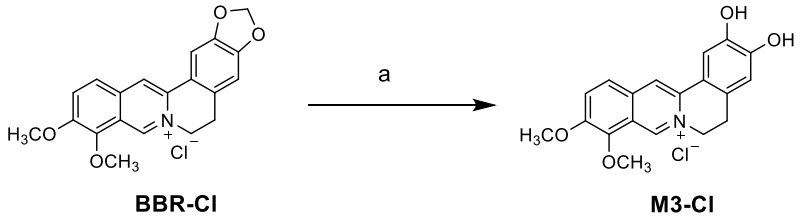

(a) 1, H_2SO_4 60%, phloroglucin, 2h, r.t.

Figure 4. Synthesis of demethyleneberberine (M3)

^{1}H-NMR (DMSO-d_6, 400 MHz): δ 3.18 (t, 2H, J= 6.0 Hz), 4.12 (s, 3H), 4.15 (s, 3H), 4.96 (t, 2H, J= 6.0 Hz), 6.91 (s, 1H), 7.60 (s, 1H), 8.11 (d, 1H, J= 8 Hz), 8.23 (d, 1H, J= 8 Hz), 8.82 (s, 1H), 9.45 (br s, 1H), 9.89 (s, 1H), 10.23 (br s, 1H). 13C-NMR (DMSO-d6, 100 MHz): δ 25.8, 55.6, 57.1, 61.9, 112.7, 114.9, 117.8, 119.3, 121.2, 123.5, 126.7, 127.2, 133.3, 138.3, 143.5, 145.1, 145.6, 149.2, 150. MS (ES): m/z 324 ($M+H^+$).

1.1.4.3 Liquid chromatography and mass spectrometry

The HPLC system used is a 2690 Alliance system (Waters, Milford, MA, USA) combined with a triple quadruple mass spectrometer QUATTRO-LC (Micromass; Waters) using an electrospray interface (ES). Analytical separation was achieved using a Phenomenex Luna C18 (5 µm, 150 mm × 2.0 mm i.d.) column.

1.1.4.3.1 HPLC optimization

The mobile phase used to achieve a good separation between berberine and its metabolites was 10 mM formic acid in water adjusted to pH 4.0 with ammonia (solvent A) and a solution of acetonitrile: methanol = 95:5 v/v (solvent B) using a gradient elution (5 min at 95% A and 10 min at 40% A, 5 min at 20% A, 10 min at 0% A) at 0.15 mL min^{-1} flow rate. The analytical column was maintained at 30°C and the sample volume injected was 10 µL.

In the optimized analytical conditions, the mean retention times were for BBR 10.0 ± 0.2 min, M1 10.4 ± 0.2 min, M3 9.2 ± 0.2 min, and M4 9.8 ± 0.2 min (n = 20). The reconstruction ion chromatogram (RIC) for BBR and its metabolites is reported in **Figure 5**.

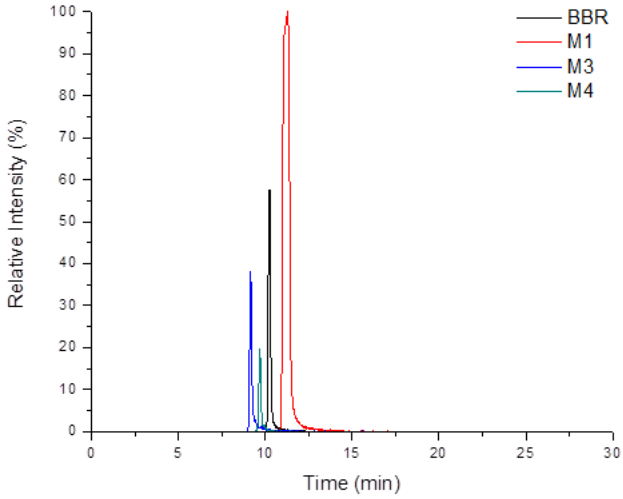

Figure 5. Reconstructed ion chromatogram of BBR, M1, M3 and M4.

1.1.4.3.2 ES mass spectrometry optimization

The HPLC was coupled to a electrospray source (ES) operating in positive ion mode, connected to a triple-quadruple mass spectrometer. For each analyte a standard solution (0.1 g/mL in 10 mM formic acid (pH 4.00): methanol 50:50 (v/v), flow of 20 L

min^{-1}) was directly infused into the mass spectrometer to find the optimal tuning parameters, reported in

Table 1.

Table 1. Tuning parameters BBR and its metabolites

Instrumental parameters	BBR	M1	M3	M4	IS
Ionization mode	+	+	+	+	+
Capillary voltage (kV)	3.3	3.3	3.3	3.3	3.3
Cone voltage (V)	44	47	44	43	42
Source temperature (°C)	130	130	130	130	130
Desolvation temperature (°C)	410	410	410	410	410
Nebulizer rate (L/h)	65	65	65	65	65
Desolvation rate (L/h)	1065	1065	1065	1065	1065
RCE (%) [a]	30	30	30	30	30
Collision gas	Ar	Ar	Ar	Ar	Ar
Parent ion (*m/z*)	336	322	324	338	414
Daughter ion (*m/z*)	320	307	280	323	220

[a] Relative collision energy

Detection was performed by Multiple Reaction Monitoring (MRM) operating in the positive ionization mode, by monitoring the transitions at m/z 336→ 320 BBR), m/z 322→ 307 (M1), m/z 324→ 280 (M3), m/z 338→ 323 (M4), and m/z 414→ 220 ((R,S)-noscapine).

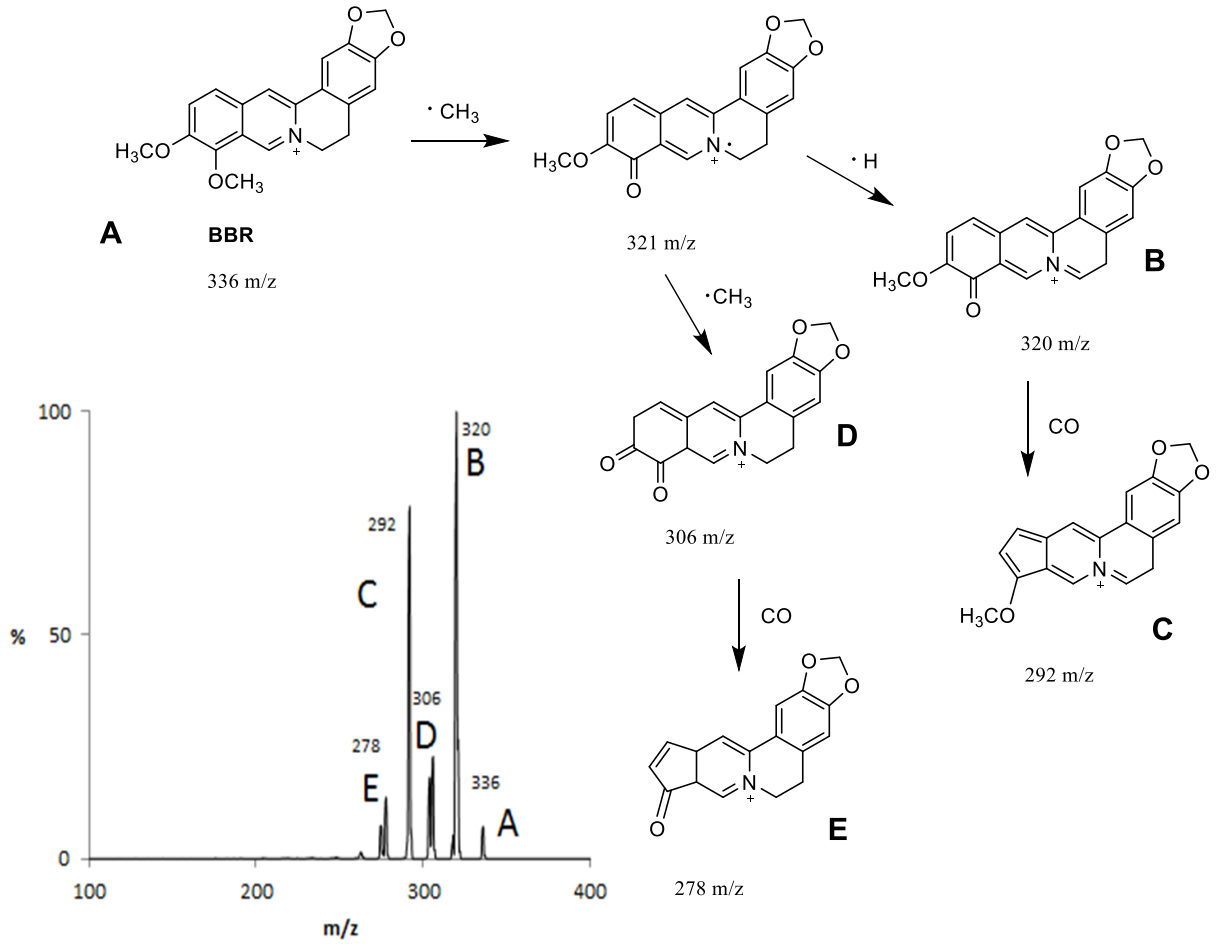

Figure 6. Mass spectra of berberine and its fragmentation scheme

1.1.4.3.3 Method validation

The developed HPLC-ES-MS/MS method was validated according to the current guidelines[15] used in drug analysis. The required validation parameters, *i.e.,* specificity, limit of detection and quantification, linearity range, accuracy and precision are reported below.

Specificity

The HPLC-ES-MS/MS method developed presents a high specificity because compounds of closely related structures, as BBR and its metabolites are discriminate by different retention times and mass spectra.

Limit of detection and quantitation

Limits of detection (LOD), estimated as the signal-to-noise ratio (S/N) equal to 3, was 0.08 ng/mL for each analyte. The limit of quantification (LOQ), estimated as S/N equal to 9, is 0.5 ng/mL for each analyte.

Linearity range

Linearity was studied in the range from 0.5 to 20 ng/mL for each analyte.

Linear calibration curve parameters were obtained from the plot of the analyte peak area/internal standard peak area versus analyte concentration using a least squares regression analysis (weight = $1/x^2$). Plasma calibration curve of BBR and its metabolites, expressed as y= (a ± DS)+ (b ± DS)x, was reported in **Table 2**. The performance of the analytical method was monitored using three quality control samples (QCs) having 4.5 nM for QC low, 20 nM for QC med and 45 nM for QC high.

Table 2. Calibration curves of BBR and its metabolites in plasma

Analytes	y= (a ± DS)+ (b ± DS)x	R^2
BBR	y= (-0.0133 ± 0.0001) + (0.339 ± 0.055)x	0.993 ± 0.005
M1	y= (-0.050 ± 0.004) + (0.809 ± 0.055)x	0.990 ± 0.003
M3	y= (-0.018 ± 0.005) + (0.159 ± 0.024)x	0.991±0.001
M4	y= (-0.0014 ± 0.0008) + (0.095 ± 0.051)x	0.994±0.001

a= intercept; b=slope; x= concentration (ng/mL); DS=standard deviation; R^2= coefficient of determination

Accuracy and precision

Accuracy (bias %) and precision (coefficient of variation, CV %) were determined intra-day, evaluated during the same day, and inter-day, evaluated during three days, using the triplicate analysis of the QCs for each analyte (

Table 3).

Table 3. Accuracy (bias %) and precision (CV %) of BBR and its metabolites

	Accuracy and precision								
		BBR		**M1**		**M3**		**M4**	
	C (nM)	**CV%**	**bias%**	**CV%**	**bias%**	**CV%**	**bias%**	**CV%**	**bias%**
Intra-day	4.5 (QC low)	9	7	7	2	8	1	7	7
	20 (QC med)	**2**	**3**	**2**	**1**	**8**	**1**	**4**	**1**
	45 (QC high)	1	1	3	2	5	2	3	4
Inter-day	4.5 (QC low)	**7**	**5**	**7**	**1**	**7**	**7**	**11**	**5**
	20 (QC med)	5	1	4	1	4	1	3	1
	45 (QC high)	**2**	**3**	**1**	**3**	**3**	**2**	**1**	**3**

Recovery and matrix effect

The extraction efficiency of solid phase extraction was expressed as recovery. The recovery % was > 90 % for each analyte while the matrix effect was < 10%.

1.1.4.4 Physicochemical properties

Determination of pKa values

The pKa values were determined in silico using Epik module version 2.2 from Schrödinger Suite 2010, setting water as solvent and using the maestro interface of Schrödinger Suite 2010 (Maestro, version 9.1, Schrödinger, LLC, New York, NY, 2010) to build all molecules.

Determination of water solubility

The solubility was experimentally determinated in Na phosphate buffer 0.1 M from pH 4.5 to 9 for each analyte under continuous stirring at 25 °C, for 1 week. Then, each solution was filtrated on RC membrane 0.45 µm syringe filters and injected in HPLC-ES-MS/MS after an appropriate dilution with mobile phase.

Determination of 1-octanol/water partition coefficient

The determination of 1-octanol/water partition coefficient was experimentally determinated in Na phosphate buffer from pH 4.5 to 9.0 for each analyte. Briefly, for each analyte 2mL of a standard solution (0.1 mM) in Na phosphate buffer, presaturated with 1-octanol, was added to 2 mL of 1-octanol (presaturated with Na phosphate buffer). The system was left to equilibrate for 1 week under continuous stirring at 25 °C. Then, the two phases were carefully separated by centrifugation. The aqueous solution was appropriately diluted with mobile phase and injected in HPLC-ES-MS/MS.

Determination of albumin binding association constants

The determination of albumin binding association constants (K_B) were performed using bovine serum albumin (BSA) 10 µmol L^{-1} in Tris-HCl buffer solution (0.05 mol L^{-1} Tris, 0.15 mol L^{-1} NaCl, pH 7.4) by fluorescence quenching. The emission spectra was obtained recording the increasing concentrations of quencher (Q: BBR, M1, M3, M4) from 0 to 24 µmol L^{-1} (increments of 2 µmol L^{-1}) setting the excitation at 295 nm and emission wavelengths of 300-500 nm.

The experimental results published on BBR quenching mechanism of fluorescence of indicate that it's a static quenching procedure[16]. For this reason, the binding association was determinated by plotting modified Stern-Volmer equation (**Figure 7**).

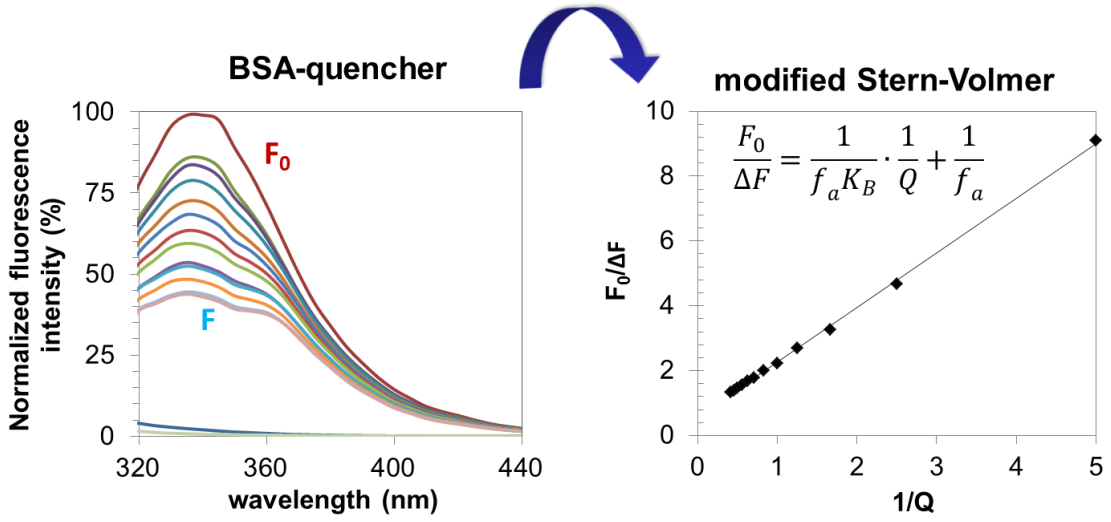

Figure 7. BSA emission spectra in presence of quencher (left) and modified Stern-Volmer plot (right)

where:

F_0 – fluorescence intensity in absence of quencher

ΔF – difference in fluorescence in absence and presence of quencher

f_a – fraction of accessible fluorescence

K_B – effective quenching constant for the accessible fluorophores

Q – concentration of quencher

1.1.4.5 Pharmacokinetics and bioavailability of berberine in human

The same formulation of Berberis Vulgaris enriched extract (250 mg cps) was acutely and chronically administered to human subjects in order to better understand berberine pharmacokinetics and the biodistribution.

The pharmacokinetics study was carried out by administering 500 mg of berberine to healthy subjects (n=10). Plasma samples were collected at different times after 1, 2, 3, 4, 6, 8, 24 h respectively.

Concerning the subchronic bioavailability study, hypercolesterolemic patients (n=12) received 15 mg/kg daily of berberine for three months (from a minor daily dose of 3 cps/day to a maximum daily dose prescribed 6 cps/day). Patient inclusion criteria were as follows: age 18 – 70 year-old; c-LDL>130 mg/mL and <190 mg/mL; fasting glucose<100 mg/mL. Total cholesterol, c-LDL, c-HDL, triglycerides, was evaluated before enrollment (V0) end after three month of berberine chloride chronically administered (V3) to evaluate the hypolipidemic effect of berberine.

These studies have been approved by the Ethical committee of the S.Orsola University Hospital (Review Board No. 7-2209-U-SPER).

1.1.5 Results and discussion

1.1.5.1 Physicochemical properties

The physicochemical properties of berberine and its metabolites, including pKa, solubility, lipophilicity and albumin binding, are reported in **Table 4**.

pKa

In silico, the pKa prediction is possible only for molecule containing proton donor or acceptor groups. For this reason the determination of pKa was performed only for berberine metabolites and no for berberine, assuming that its iminium cation would remain as such in all pH range.

The simultaneous presence of the iminium cation and the hydroxyl group in the structures of berberine metabolites play a crucial role. Indeed, these compounds could take on the characteristics of neutral molecules when pH is higher than the pKa value. Specifically, M3 and M4 are partially dissociated in physiological pH, having a pKa value 9.4 and 9.6 respectively. No pKa value was retuned for M1 as the most stable tautomer in water was its neutral quinoid form.

In order to demonstrate the keto-enolic equilibrium of M1 (**Figure 8**), its quinoid form was synthetized and an NMR study was performed.

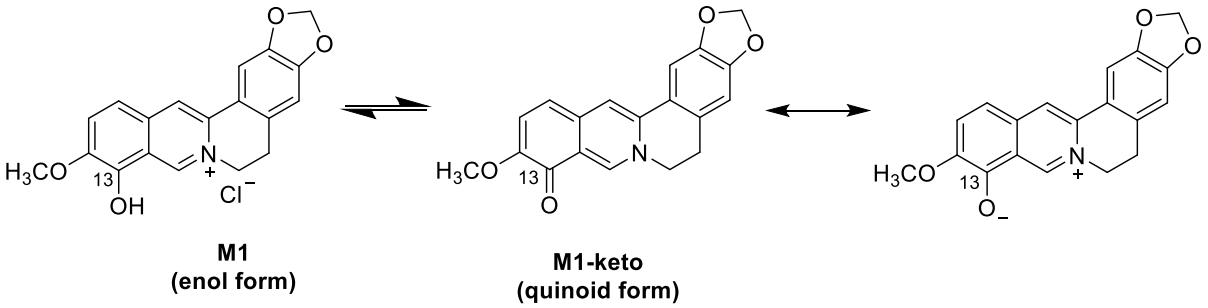

Figure 8. Keto-enolic equilibrium of M1

Water solubility

As show in Table 4, the solubility of berberine was not influenced by pH variation while the solubility of M3 and M4 increased significantly when pH was increased. Concerning M1, its solubility decreased when pH was increased and the color of M1 in solution turned from yellow at acidic pH to red a basic pH. This bathocromic effect could be due to prevalence of enolic form at low pH and quinoid form M1-keto at high pH, as previously hypothesized.

Lipophilicity

The coefficient partition 1-octanol/water (LogPo/w) of berberine and its metabolites are reported in **Table 4**.

Unlike its metabolites, the LogPo/w of BBR is not greatly influenced by pH because in its structure there are not proton donor or acceptor functional groups. Thus the only species present in its solution, at each pH value, is BBR as such (**Figure 1**).

BBR, M3 and M4 could be classified as hydrophilic compounds (LogPo/w<0) while conflicting data are obtained for M1.

The lipophilicity of M1 is strongly influenced by pH variation, increasing with increasing pH from Log -0.02 to 1.6. This latter value is in disagreement with its nominal enolic structure indeed M1 should be more hydrophilic than berberine. This M1lipophilicity variation could be attributed to the predominance of the enol form (total positive charge) at acid pH (4.5) and the quinoid form at basic pH (total neutral charge), that is more liposoluble. Indeed, as seen in solubility assay, a different phase color was observed during the partition in 1-octanol and aqueous medium of M1: yellow in aqueous phase and red in 1-octanol (**Figure 9**).

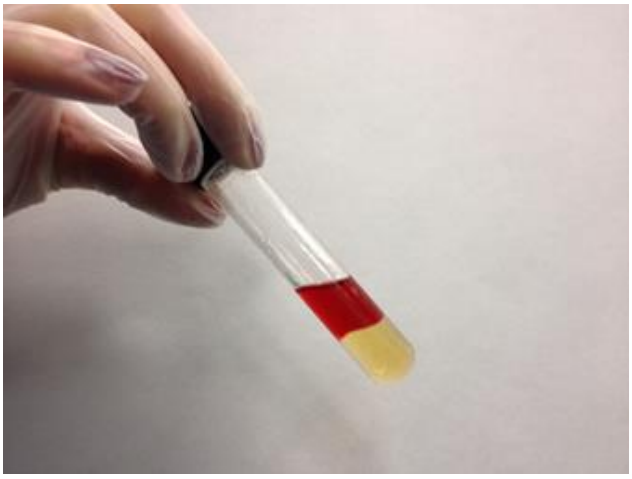

Figure 9. Coefficient partition 1-octanol/water of M1

Albumin Binding

In **Figure 10** the tryptophan fluorescence quenching effects induced by berberine, M1, M3 and M4 respectively are reported. The presence of a double peak in quenching profile of BBR, M3 and M4, suggest that they bind both binding sites of BSA. On the

other hand, the quenching profile of M1 is characterized by a single peak suggesting that this metabolite bind only one sites of BSA. The affinity constants binding are reported in **Table 4.**

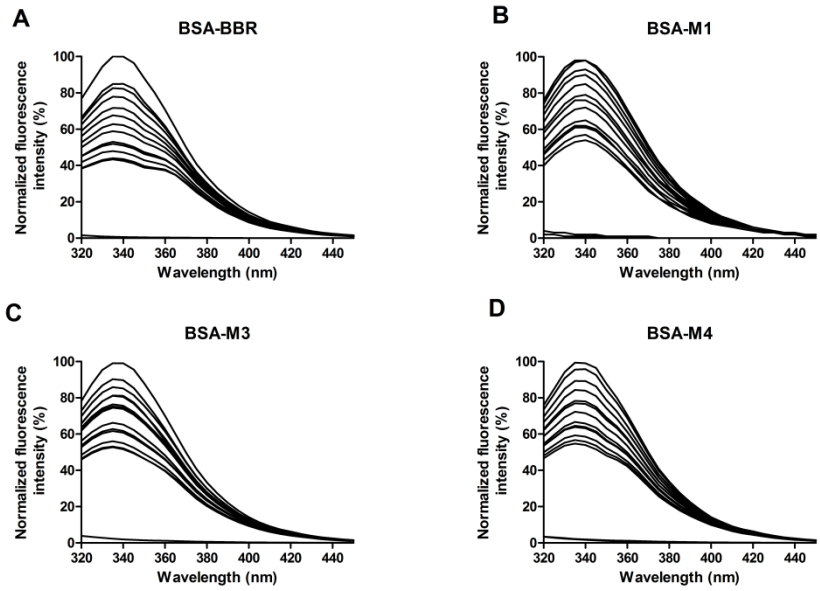

Figure 10. Emission spectra of BSA (0.1 μM) at different concentrations of: (A) BBR, (B) M1, (C) M3, and (D) M4 (λext = 280 nm)

Table 4. Physicochemical properties of BBR and its metabolites

Compound	pH[a] gradient	Solubility (mM)	LogPo/w[a]	LogDo/w	K_B[b] (x10^3 L·mol^{-1}) ± SD
BBR	8.6	9.6	-1.2	-1.2	3.37 ± 0.09
	7.0	9.0	-1.2	-1.2	
	6.0	7.6	-1.2	-1.2	
	4.5	8.2	-1.2	-1.2	
	in silico	-	-0.4	-	
M1	8.6	0.5	1.6	4.6	1.51 ± 0.03
	7.0	1	1.1	2.5	
	6.0	2	0.9	1.4	
	4.5	4.2	-0.02	0.01	
	in silico	-	1.0	-	
M3	8.6	6.5	-0.5	-0.3	1.98 ± 0.09
	7.0	3.7	-1.1	-1.1	
	6.0	0.2	-1.1	-1.1	
	4.5	0.2	-1.1	-1.1	
	in silico	-	0.1	-	
M4	8.6	12.2	0.1	0.6	1.73 ± 0.01
	7.0	12.4	-1.2	-1.2	
	6.0	1.3	-1.5	-1.5	
	4.5	1.5	-1.5	-1.5	

[a]phosphate buffer 0.1 M. [b]at 298 K in 0.1M Tris-HCl pH = 7.2 (n.d.= not determined). [c]Chloride salt

1.1.5.2 NMR characterization of berberrubine

In order to demonstrate the keto-enolic equilibrium of M1, NMR spectroscopic studies have been performed. In particular, the NMR characterization was carried out for a equimolar mixture of enol and quinoid form of M1, using several NMR spectroscopic technique. Specifically, the ^{1}H-NMR spectra of this equimolar mixture displayed only one average set of signals, confirming that a fast equilibrium between this two tautomeric forms take place.

In addition, a ^{1}H-^{15}N HMQC (recorded at 40° C in DMSO-d_6) correlation analysis was carried out for both structures. In the NMR of enol form, correlations of H8 triplet and the H11 singlet with N10 resonance at 193 ppm were observed. As expected, the same correlations (**Figure 11**) of H8 triplet and the H11 singlet with N10 were obviously observed for quinoid form while N10 resonance was found at 164 ppm. The difference between the chemical shifts for the two ^{15}N resonances is due to the different electron density of quaternary N atom in enol form and that of tertiary N atom in quinoid form.

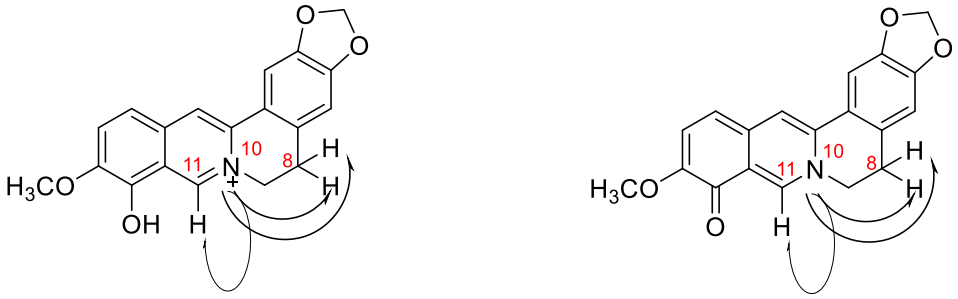

Figure 11. 1H-15N HMQC correlations for the enol form and quinoid form

1.1.5.3 Plasma sample extraction and clean up

Analytes were extracted from plasma using an Oasis HLB (hydrophilic−lipophilic balance 200 mg, 6 mL) SPE column. The optimized extraction procedure utilized: conditioning with 2 mL of MeOH and 2 mL of H_2O Milli-Q; loading with 100 µL of plasma (+10 µL of IS, 10 ng/mL) diluted with 2 mL of ammonium formiate (10 mM pH 7.0), washing with 1 mL of formic acid (2%, v/v) and 2 mL of ammonium formiate (10 mM pH 7.0), elution with 2 mL of MeOH, followed by 1 mL of MeOH containing 1% (v/v) CH_3COOH and 1 mL of MeOH containing 2% (v/v) NH_4OH, vacuum drying, and reconstitution with 100 µL of mobile phase. The recovery percentage was ≥90% for all analytes.

1.1.5.4 Pharmacokinetics and bioavailability of berberine in human

In **Figure 12** are reported plasma levels of BBR and its metabolites after acute and chronic administration.

Concerning the pharmacokinetic study, the curve of BBR, M3 and M4 are quite similar. Their maximum plasma concentration are very low, i.e. 0.07 ± 0.01 nM for BBR, 0.14 ± 0.01 nM for M3, and 0.13 ± 0.02 nM for M3. Instead, plasma levels of M1 reach a maximum concentration of 1.4 ± 0.3 nM, ten times higher than BBR and others metabolites.

After chronic administration (**Figure 12**), a bioaccumulation of BBR and its metabolites was observed. The steady-state levels were 4.0 ± 2.0 nM, 6.7 ± 3.0 nM, 1.7 ± 0.3 nM, and 5.6 ± 2.0 nM for BBR, M1, M3 and M4 respectively.

These plasma levels are higher than those after acute administration because the dose was twice compared to acute one.

In

Table 5 the comparison of cholesterol (total, LDL and HDL) and total triglycerides before (V_0) and after the treatment with Berberine chloride for three months (V_3) was reported.

Among biochemical-marker of hypercholesterolemia, a significant reductions in total and LDL cholesterol ($p<0.05$ obtained by the paired two-tailed Student's t test) was observed and this is in agreement with previously published data[17]. In contrast, total triglyceride and cholesterol-HDL levels were not significantly different ($p>0.05$) before and after chronic administration of BBR.

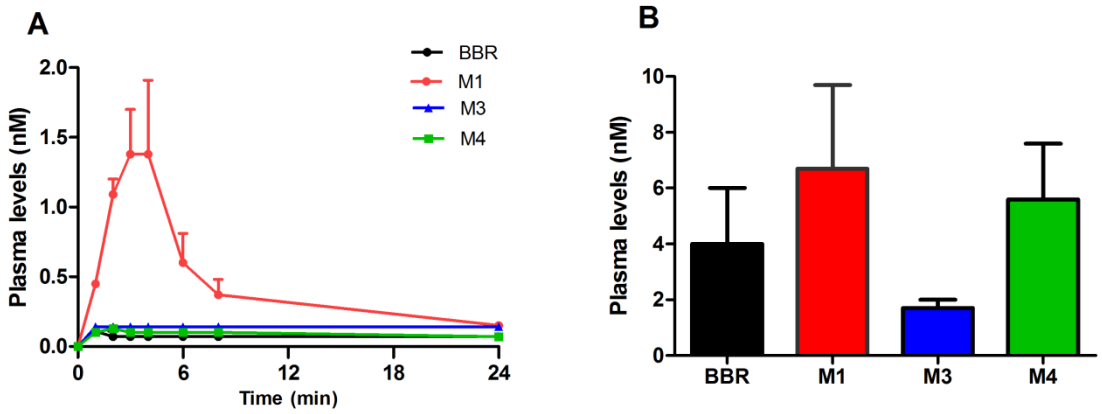

Figure 12. Plasma levels of BBR, M1, M3 and M4 (A) acute administration of BBR 500 mg (n=10) (B) chronic administration of of BBR 15 mg/kg

Table 5. Biomarkers of hypercholesterolemia before (V_0) and after the treatment with Berberine chloride (V_3)

Patient	total-cholesterol (mg/dL)		LDL (mg/dL)		HDL (mg/dL)		triglycerides (mg/dL)	
	V_0	**V_3**	**V_0**	**V_3**	**V_0**	**V_3**	**V_0**	**V_3**
1	268	233	173	138	65	59	134	179
2	238	251	162	181	50	51	119	87
3	193	205	133	138	35	36	113	156
4	196	147	131	90	51	46	63	48
5	211	187	136	115	45	43	133	132
6	211	200	132	111	69	70	47	87
7	201	188	126	111	48	51	120	118
8	241	227	174	158	39	37	126	162
9	276	267	194	197	48	46	168	110
10	229	226	145	141	56	58	128	123
11	213	182	137	124	38	37	190	95
12	225	210	149	137	49	49	122	118
P	0.016*		0.025*		0.312		0.753	

p= paired two-tailed Student's t test

1.1.5.5 Correlation between plasma levels and physicochemical properties

Among the physicochemical properties studied for BBR and its metabolites, the pKa and the lipophilicity are correlated with plasma levels after oral administration. As previously reported, pKa values showed that BBR, M3, and M4 were permanently charged at the physiological pH range while M1 tautomerized in its neutral quinoid form (**Figure 13**).

This keto-enol tautomeric equilibrium was strongly influenced by pH and the two forms of M1 (i.e. enol and quinoid form) interconvert rapidly into each other. Likely, the prevalence of its enolic form or quinoid form was continuously modulated in vivo and their separation could be promoted by a membrane in systemic compartment. The intestinal adsorption of quinoid form could be more efficient than enol form because a neutral molecule cross much better membranes than a charged one (**Figure 13**).

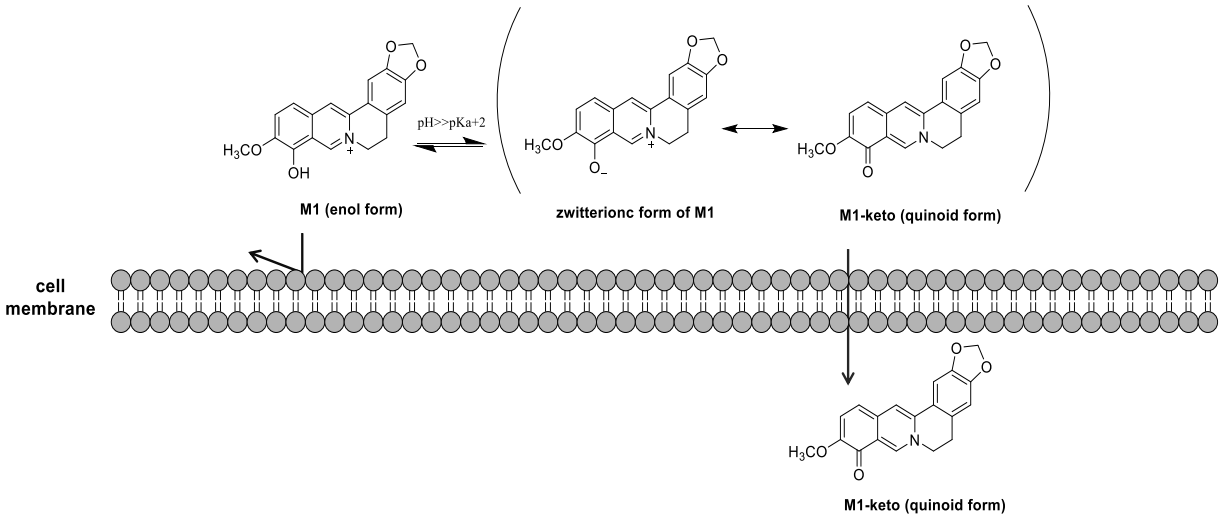

Figure 13. pH-mediated passive diffusion of M1 through the cell membrane

Summarizing, BBR has an unusual metabolism through it produces a metabolite, M1, more lipophilic than BBR in its quinoid form. For this reason, it was hypothesized that M1 could be adsorbed by passive diffusion and this accounts for its higher plasma

levels. Thus M1 accumulates in systemic compartment more than BBR and other metabolites and as discussed above, M1 seems to be more pharmacologically active but this hypothesis should be demonstrated by the direct administration of M1.

1.2 Berberrubine

1.2.1 Pharmacological and therapeutic effects

As reported above, M1 showed a cholesterol-lowering efficacy, although its activity was lower than BBR (about 40% lower). In order to improve the low bioavailability of BBR, several prodrugs of M1 were designed, in which the 9-hydroxl group of M1 was replaced with different ester groups. Consequently its cholesterol-lowering effect is increased because these new compounds are more lipophilic than M1 and BBR[18].
In addition, recent studies have been demonstrated that berberrubine exhibits anti-tumor activity in animal models. In particular, M1 exhibits an antitumor activity higher than BBR, due to the hydroxyl group at the 9-position in the M1 structure. The substitution of the methoxy group in BBR structure with an hydroxyl group in M1 could mediate DNA cleavage by topoisomerase II[19,20].

1.2.2 Aim and rationale

Despite its significant pharmacological effect, the bioavailability of BBR (**Figure 1**), obtained by the area under the curve and maximum concentration in blood, was less than 1%. BBR is an isoquinoline alkaloid isolated from several Chinese herbal medicines, such as Coptis chinensis, Berberis aristata, and Coptis japonica that exhibits a multi-taget activity. In particular a lipid-lowering effect by up-regulating the hepatic low density lipoprotein receptor (LDLR) expression is obtained after oral

administration of 500mg/die of berberine chloride. As well as BBR, also its primary metabolites showed a cholesterol-lowering effect although less than BBR activity.

Recently, several studies[21] have been carried out to explain how this molecule so poorly bioavailable exhibits these important pharmacological activities. In particular, the biodistribution of BBR and its metabolites in main organs or tissues was further investigated. After oral administration a dominant tissue distribution of BBR and its metabolites was observed in the liver. This pharmacological result has been used to explain why BBR is active in vivo, even if its blood concentration is low. Indeed, the authors have been hypothesized that an accumulation of BBR and its metabolites could explain their therapeutic effect on cholesterol, glucose and triglycerides in patients.

Although the bioavailability of BBR is low, the concentration of M1 in blood was ten times higher than BBR and others metabolites (as reported below). For this reason M1 could be potentially more pharmacologically active than berberine.

Previously we have demonstrated that M1 could tautomerized in its quinoid form which could accumulate in systemic compartment more than BBR.

In order to demonstrate the tautomeric equilibrium in vivo of M1, in vivo experiments on "rat with external biliary fistula" were carried out. Specifically, M1 will be duodenal administered at 10mg/kg. Plasma, liver and bile will be collected during all the experiment. Then, the biodistribution of M1 will be compared with BBR.

For this purpose it will be necessary to develop and validate clean up procedures for the extraction and purification of analytes by these matrices.

1.2.3 Experimental

1.2.3.1 Materials and reagents

Wistar-Han rats (male, 180–220 g, 6–7 weeks) for the following pharmacokinetic study were obtained from Charles River Laboratories, Carlo, Italy. All the experiments were conducted following relevant National and International Guidelines according to Public

Health Service Policy on Humane. The animals were maintained on a 12-h light/dark cycle (light on from 8:00 AM to 8:00 PM) at ambient temperature (22–24 °C) with 45% relative humidity. The rats were fasted for 12 h before all experimental studies.

1.2.3.2 Comparison between pharmacokinetics and biodistribution of berberine and berberrubine in bile fistula rat animal model

The animal model used was the bile fistula rat in which, the bile duct was cannulated to collect the bile at time interval after intraduodenal administration of the compound per gavage. Berberine and M1 were infused at a dose of 500 nmol/kg/min (10mg/kg) over 2 hour at 2.5 ml/hour.

Bile was collected at 15 minutes time intervals throughout the infusion and over 2 hours after the infusion was over while plasma was collected every 30 minutes and liver at the end of experiment. The bile flow was evaluated gravimetrically by the volume of bile recovered at the different time-intervals, while the concentration of the administered compounds and its main metabolites were measured in bile, plasma and liver samples with the HPLC-ES-MS/MS as reported below.

In the anesthetized animal, the intestinal motility is hampered not allowing the progression of the substance. For this reason an intraduodenal infusion was preferred over the single bolus infusion in which the absorption would be disturbed by the absence of luminal stirring.

1.2.4 Results and discussion

1.2.4.1 Sample extraction and clean-up procedures: bile and liver

Bile Sample Preparation

Rat bile samples were brought to 25°C and diluted 1:10000 v/v with ammonium formiate buffer 10 mM pH 4.0 and acetonitrile–methanol (95:5 v/v) in ratio 95:5 (v/v) and 5 µl was injected in HPLC-ES-MS/MS system.

Liver Sample Preparation

Aliquots weighing approximately 1 g each were taken from different points of the liver sample. Each aliquot was weighed, and 2 ml of phosphate buffer (0.005 M, pH 7.2) was added. The mixture was homogenized using a potter, which was then washed with 3 mL of methanol. The liver extract was sonicated for 5 minutes, vortexed for 2 minutes, heated to 37°C for 20 minutes, and centrifuged at 2100g for 15 minutes. Four hundred microliter of the supernatant was spiked with 10 µl of the internal standard working solution and dried under vacuum. The residue then was re-suspended with 2 ml of ammonium formiate (10 mM pH 7.0) and SPE was carried out on HLB extraction cartridges (as shown above). The eluate was dried under vacuum and reconstituted with 200 ml of the mobile phase) and injected into the HPLC-ES-MS system.

1.2.4.2 Metabolism of berberrubine

The metabolism of berberine has been further investigated, and M1, M2, M3 and M4 were identified as main primary metabolites (**Figure 1**).

In this work, it was hypothesized that, as well as berberine, M1 might be further metabolized in the liver by CYP450 isoenzymes through oxidative demethylation at positions 2, 3, 9, and 10 followed by conjugation of these hydroxyl group functions with glucuronic acid. The hypothesized primary metabolites of M1 were reported in **Figure 14**.

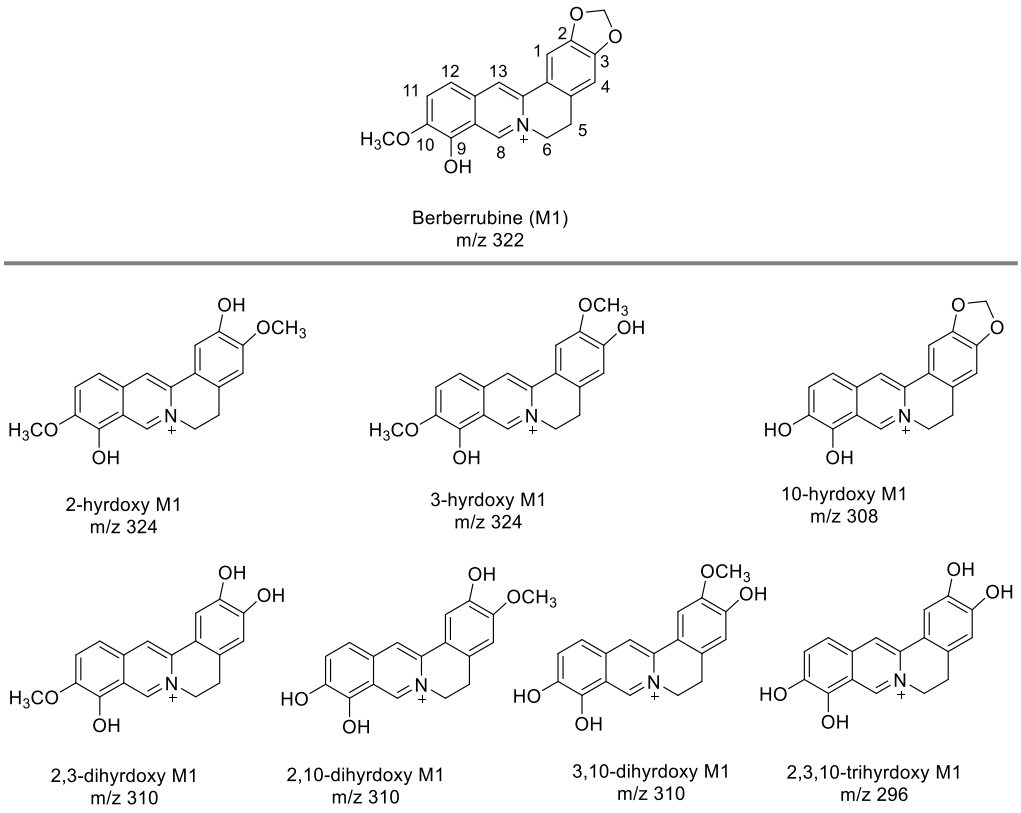

Figure 14. Primary metabolism of M1

1.2.4.3 Comparison between pharmacokinetics and biodistribution of berberine and berberrubine

The bile flow and bile secretion of M1 (A) and BBR (B) are reported in **Figure 15** and **Figure 16**. After duodenal infusion of M1 and BBR, a reduction of bile flow was observed for each compound, reaching a minimum volume secretion (SVmin) of 20 and 2.9 µL/min/kg for M1 and BBR respectively. The bile flow reduction could be due to the animal model chosen in which the enterohepatic circulation was interrupted.

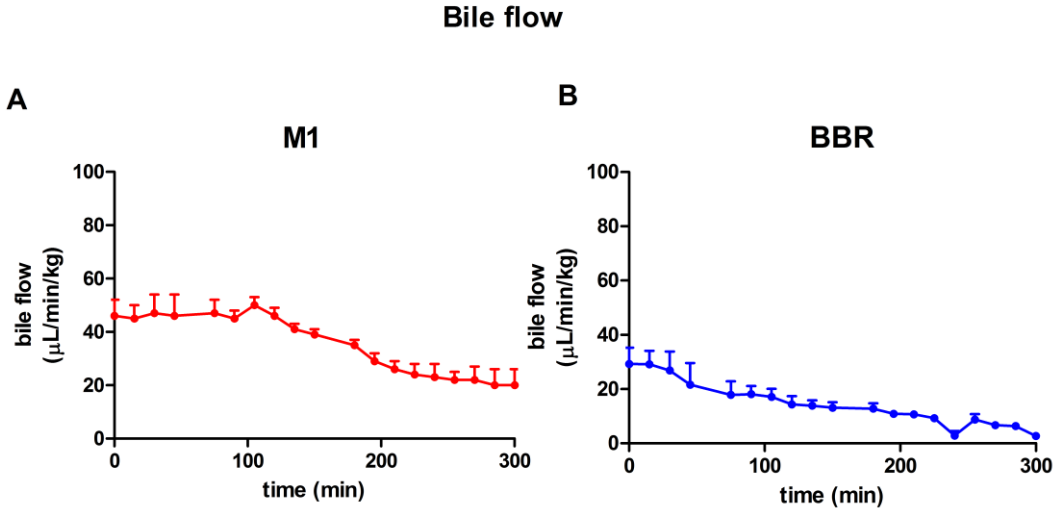

Figure 15. Bile flow of A) M1 and B)BBR

Concerning their biliary secretion, it is more efficient for M1 than BBR. Indeed, the maximum bile secretion (SBmax) of M1 is 6 times higher than BBR SBmax (*i.e.* 19.6 and 3.3 nmol/ min/ kg). In bile M1 was poorly metabolized to mono and dihydroxyl derivatives while BBR was metabolized in M1, M3 and M4 (SBmax i.e. 1.3, 1.2 and 1.2.nmol/ min /kg).

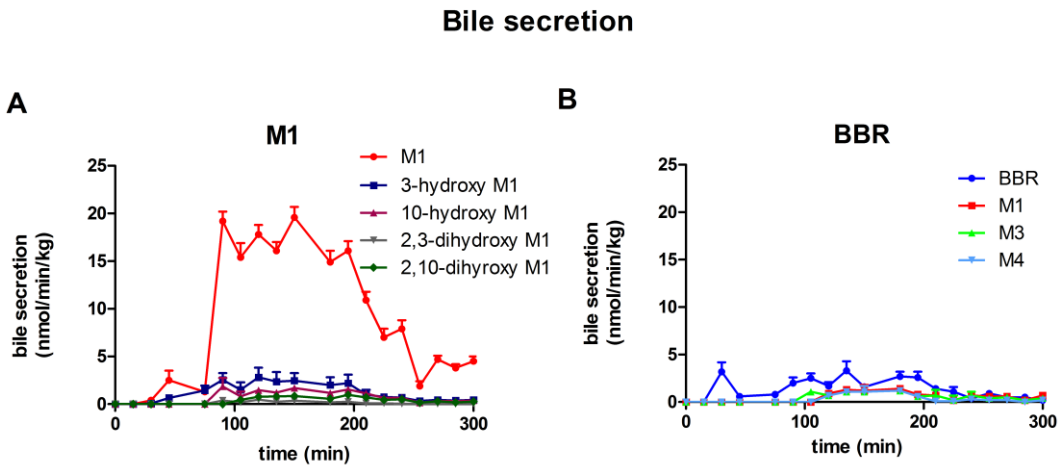

Figure 16. Bile secretion of A) M1 and B) BBR

Plasma profiles of M1 and BBR were reported in **Figure 17**. As expected, the bioavailability of BBR is very low, reaching a maximum plasma concentration (Cmax) of 0.046 µM after 240 min. In particular, after duodenal infusion of BBR, it is mainly metabolized to M1 (Cmax 0.085 µM after 120 min) and less to M3 and M4 (*i.e.* 0.05 and 0.025 µM). Differently from BBR after duodenal infusion, M1 was poorly metabolized reaching a Cmax of 11.8 µM after 240 min.

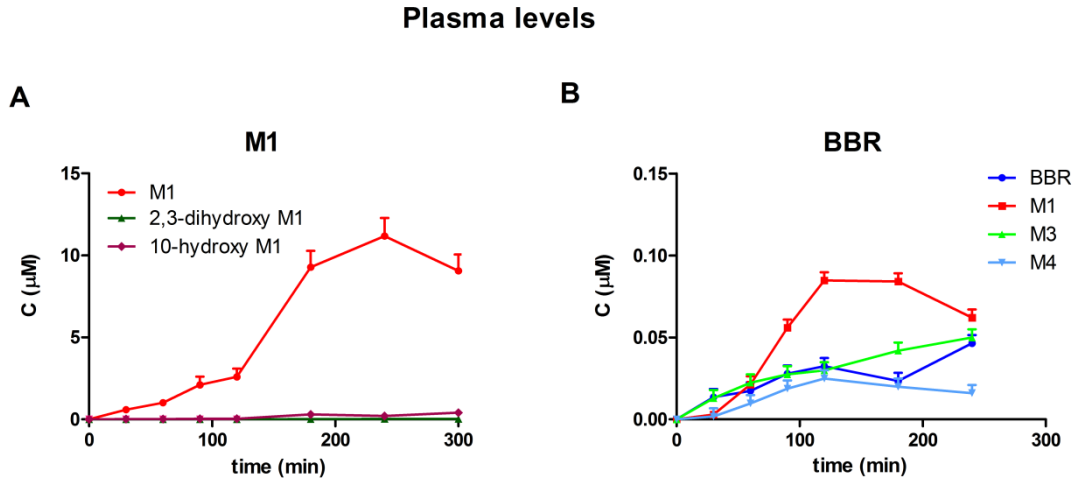

Figure 17. Plasma levels of A) M1 and B) BBR

In liver, the amount of M1 was 52 nmol/g after its direct administration and no metabolites were detected. Unlike, after duodenal infusion of BBR, the amount of BBR

was 34.4 nmol/g, 26.5 nmol/g for M1, 1.6 nmol/g for M3 and 8.4 nmol/g for M4 respectively.

1.3 Conclusions

The physiochemical properties of BBR and of its metabolites showed that it has an unusual metabolism as its metabolite M1 is more lipophilic than BBR. Indeed the nitrogen atom of M1 structure could be tetravalent with a positive charge in its enol form and trivalent and electroneutral in quinoid form (**Figure 13**) by keto-enol tautomerism equilibrium unlike BBR and the other metabolites. It was hypothesized that the intestinal adsorption of M1 quinoid form could be more efficient than enol form because a neutral molecule cross better membranes than a charged one. In this way, M1 could be adsorbed by passive diffusion and be pharmacologically more active than BBR.

Indeed, the direct administration of M1 has shown that it is more efficiently secreted in bile than BBR with a SBmax of 19.6 and 3.3 nmol/min/kg respectively. In addition, the metabolism of M1 was widely investigated. Although, M1 was poorly metabolized unlike as observed for BBR in which the SBmax of its metabolites was 1.3, 1.2 and 1.2 nmol/min/kg for M1, M3 and M4 respectively. The main metabolites present in bile were 3-hydroxy, 10-hydroxy, 2,3-dihydroxy and 2,10-dihydroxy derivatives reaching a SBmax of 2.82, 1.87, 0.47 and 0.98 nmol/min/kg respectively.

Concerning plasma levels, M1 exhibited a higher concentration both when it was directly infused (Cmax=11.8 μM) and when it was produced by BBR (Cmax=0.085 μM, time 120 min) compared to BBR plasma levels as expected. In particular, unlike BBR (Cmax=0.046 μM), M1 was detected as such in plasma and poorly metabolized. In the liver, M1 was detected as such (52 nmol/g) and no metabolites were detected. After duodenal infusion of BBR, the same total amount reaching for M1 was observed (BBR was 34.4 nmol/g, M1 26.5 nmol/g, M3 1.6 nmol/g and M4 8.4 nmol/g).

Based on this consideration, M1 could be highly conserved in enterohepatic circulation (**Figure 18**) thought to be actively absorbed in the ileum in its quinoid form by keto-

enol tautomerism. Indeed, in the intestine (pH>6.00) the neutral quinoid form of M1 is the most abundant species. Then the quinoid form of M1 could be reabsorbed by active transport at end of small intestine resulting in a higher concentration in blood.

Studies on the relationship with biomarkers of different diseases are currently underway for M1 in enol and quinoid form.

The overall data suggest the importance of accurate preclinical studies of natural products. In particular studies on biodistribution, metabolism, and accumulation in target organs should be carried out although not required by the regulatory authorities. Moreover the metabolism and biodistribution are strongly influenced by administered dose. A lack of this information represents a serious risk for the consumers' safety. In addition, in order to improve the lead discovery for pharmaceutical research based on natural sources, a physicochemical characterization should be carried out. In this physicochemical characterization the major metabolites of biologically active compound should be included.

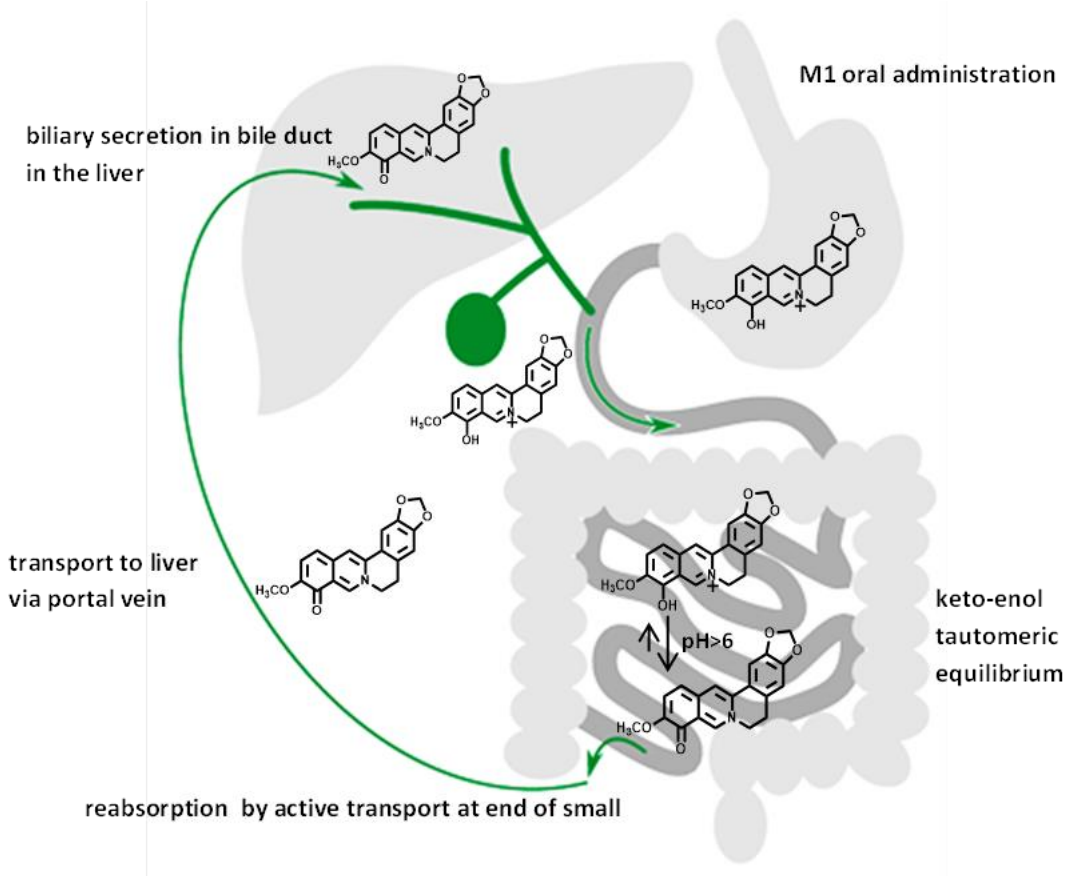

Figure 18. Enterohepatic circulation of M1

Chapter 2

Functional foods: glucosinolates

In the nutraceutical definition, functional foods are included since they are foods fortified with one or more biologically active molecules, providing a health benefit beyond basic nutrition. The depth study of foods chemical composition, such as fruits and vegetables, is a deal of great actuality for prevention, as it may lead to the discovery of new functional foods without any added cost[22].

For disease prevention, an optimization of composition of vegetables and fruits would be very cost-effective. Recognized candidates as potentially health promoting compounds, and ones which are currently under investigation in many research projects include organosulphur compounds.

The research on functional foods has focused on broccoli and on a single bioactive component within broccoli, sulphoraphane. Indeed, active components present in these vegetables, as isothiocyanates and indole-3-carbinol, showed an anticarcinogenic action has been extensively studied in experimental in vivo[22].

2.1 Glucosinolates

2.1.1 Structure and properties

Glucosinolates (GLS) are naturally occurring polar molecules classifiable as (Z) β-thioglucosides N-hydroxysulfate endowed with a lateral chain (R) and a β-D-glucopyranosil moiety linked to S-atom (**Figure 19**). GLS are produced by over sixteen plant species as Brassicaceae, Capparaceae e Caricaceae (broccoli, rocket salad, cabbage and mustard)[22]. In particular, GLS are the main responsible of organolectic properties of these vegetables.

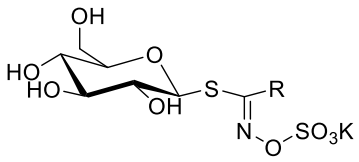

Figure 19. Structure of glucosinolates

GLS are hygroscopic, highly hydrophilic compounds having a 1octanol-water partition coefficients ranging from -1 to -3. They have a good thermostability (stable up to 110 °C in their purified form, while even more stable if in their natural matrix) and occur in nature as extremely water soluble anions. Because of the sulfate group acidity, glucosinolates are concentrated in plant vacuoles as potassium salts.

They could be classified by the chemical structure of their lateral chain in aliphatic, ω-metilthioalchylic (alifatic glucosinolates), aromatic or etherocyclic (aromatic glucosinolates) chains. Among them, many glucosinolates present linear or branched lateral chains, double bonds, carbonyl groups, hydroxyl groups and thio-groups in different oxidation states.

Glucosinolates total content in leaves is about 1% of the dry weight but its amount reaches 10% in some seeds[23]. Glucosinolates are biosynthesized starting from glucose and aminoacids[23]. Briefly, their biosynthesis is composed by three steps[24]: lateral chain elongation, glucone synthesis and structural modifications of the lateral chain.

Elongation proceeds thanks to specific genes. Once completed lateral chain elongation, biosynthesis proceeds with the N-oxydrilation, followed by decarboxylation to form an aldoxime. Such aldoxime is oxydized to tiohyroxamic acid, which is glycosylated on the S-atom obtaining a desulphoglucosinolate. Finally the desulphoglucosinolate is converted to glucosinolate thanks to the addition of a sulphate group by the action of the enzyme desulphoglucosinolate sulphatetrasferase (PAPS). Reactions modifying aminoacid lateral chain are mainly oxidation reactions on the S-atom, alchilic portions desaturation and double bond hydration.

2.1.2 Glucosinolates metabolism: isothiocyanates

Glucosinolates are hydrolyzed by myrosinase enzyme to produce a wide range of degradation products with different biological activities. Indeed, myrosinase is an endogenous thioglucohydrolase enzyme present in plants that cleaves off the glucose group from a glucosinolate with the production of thiohydroxammate O-sulphonate derivative. This intermediate decompose to several hydrolysis products: isothiocyanates (ITCs), thiocyanates, nitriles, epithionitriles, oxazolid-2-thiones and indolyl compounds (**Figure 20**). Among the degradation products of GLS, ITCs show the most important biological activity and nutraceutical applications, as reported above.

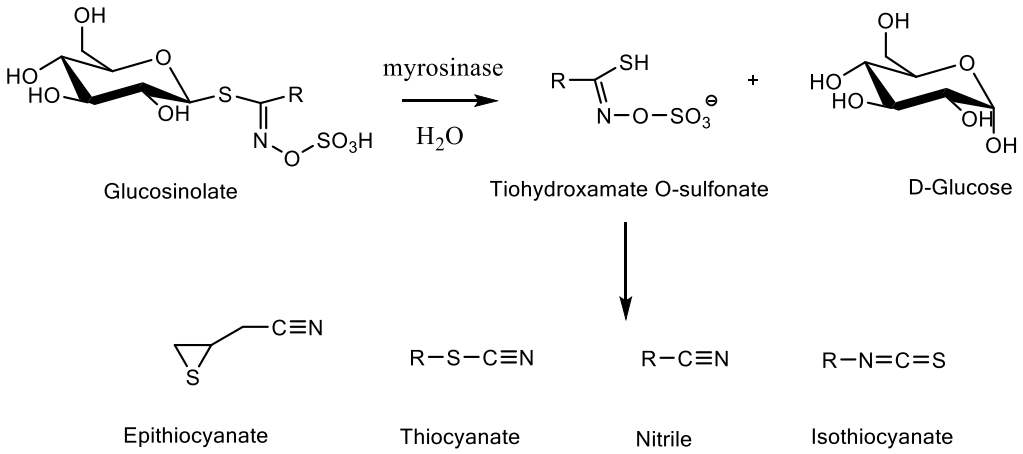

Figure 20. Glucosinolates hydrolysis

2.1.3 Biological activity and nutraceutical applications

The epidemiological evidence for cancer protection[25] associated with consumption of Brassica vegetables is attributed to the glucosinolates. However, cancer cell toxicity experiments have demonstrated that GLSs are not bioactive[25]. In contrast, their degradation products, isothiocyanates (ITCs), show important biological activity. In particular they are able to influence phase I and phase 2 biotransformation enzyme, thereby possibly influencing several processes related to chemical carcinogenesis, e.g. the metabolism, DNA-binding and mutagenic activity of promutagens[25]. Their anticarcinogenic action depends on many factors, such as the test system, the target tissue, the type of carcinogen challenge and the anticarcinogenic compound, their dosage, as well as the timing of the treatment.

In addition, ITCs showed an antinflammatory, bactericide[26], fungicide[27] and nematocide[28] activity.

By far the major ITCs well studied are erucin, sulforaphane, allilisothiocyanate, phenetilisothiocyanate and indole-3-carbinol (

Figure 21) which derive, respectively, from glucoerucine, glucoraphanin, sinigrin, gluconasturtiin and glucobrassicin.

On the other hand, negative effects of glucosinolates on animals are related to its concentration in diet. In particular, thiocyanates, thiourea and oxazolidithione may disrupt iodine availability to thyroid thus affecting thyroid function[29]. Other adverse effects of glucosinolate metabolites are goitrogenecity[30,31,32], mutagenecity, hepatotoxicity and nephrotoxicity[33,34]. The negative influence of dietary glucosinolate on animal growth and production may be related to the drastic endocrine disturbance induced by antinutritional factor[35]. The reduced intake of GLSs containing diets is due to the presence of sinigrin and progoitrin, these both glucosinolates are associated with bitter taste[36].

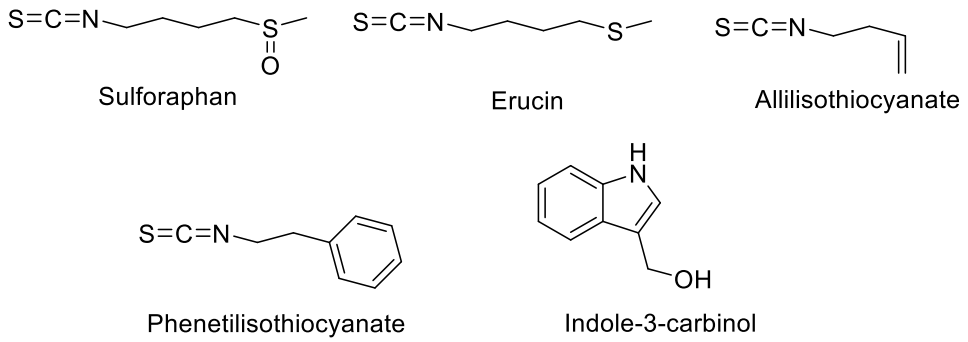

Figure 21. Glucosinolates metabolites best characterized

2.1.4 Glucosinolates and isothiocyanates determination techniques

Considering the great importance of glucosinolates, many extraction and quantitation methods have been developed.

The current analytical method for the glucosinolates is the ISO 9167-1 protocol[37] in which the glucosinolates are converted to desulphoglucosinolates (DS-GLS, **Figure 22**) using an enzymatic treatment "on column". This reaction is performed into columns filled with anion exchange resin and conditioned using an acetate buffer. After conditioning a purified sulphatase and the extracts were loaded and left for 72 hours at room temperature allowing the reaction to complete. Then, desulphoglucosinolates are eluted with water, injected into HPLC column using a C18 as stationary phase and detected by UV. For the quantification, desulphobenzylglucosinolate as internal standard, desulphosinigrin as external standard and apposite correction factors for each analyte are used. The ISO protocol, however, is an indirect analysis method whose accuracy is strictly related to the conversion yield, it is quite slow; it has low sensitivity (0.1 µmol/mL) and low selectivity[37].

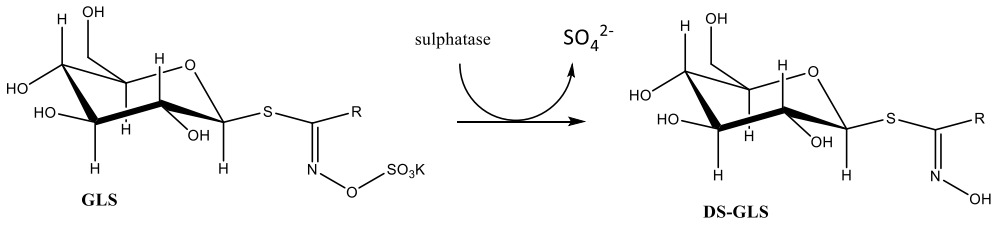

Figure 22. Glucosinolates conversion to desulphoglucosinolates

Moreover little modifications to this protocol were done but the interlaboratories data often are in disagreement to each other. Although many HPLC-ESI-MS/MS methods were developed, the ISO protocol continues to be the most popular glucosinolates analysis method. Indeed, this method is fully validated and gives satisfying results (linearity range 0.1-3 µmol/mL; precision and accuracy 12% for both).

The glucosinolates quantification was performed by GC in which GLSs were esterified by trimethylsilyl chloride, purified and injected into GC-column[38] but this way totally replaced by the introduction of new HPLC methods of analysis.

Different HPLC-ESI-MS/MS methods have been proposed, allowing new compounds discovery and the improvement of the chromatographic separations. Complex separations of many glucosinolates in vegetables matrices have been performed, up to 12 analytes, with high selectivity and accuracy[39]. However, methods for the simultaneous quantification of glucosinolates and isothiocyanates were not developed to date. This may be due to their weak absorption at UV detectors and their bad ionization in negative mode into MS sources. However the development of an efficient sample extraction and clean-up and quantitative method applicable simultaneously to both GLSs and ITCs would be of high scientific and practice interest, as it may give the opportunity to monitor GLSs stability into functional foods in relation to their hydrolysis products.

2.2 Aim and rationale

Glucosinolates and their associated degradation products have been recognized long for their distinctive benefits to human nutrition and plant defense.

Due to their beneficial effects, different functional foods were developed. Concerning GLSs, their stability during the whole industrial processing should be monitored to ensure the activity of functional foods, from cultivation to consumer processing[40]. In this way consumers will receive a functional food that is of higher nutritive quality and thus provides increased health benefits.

It was demonstrated that some GSLs and their breakdown products are to be toxic, and even carcinogenic, at high concentrations[41]. Thus, an overconsumption of these compounds could have serious health consequences[42] as high-dose−effect relationships are as yet unknown in humans[43].

The quantification of GLSs in functional foods is regulated by ISO 9167-1 procedure, based on their preliminary conversion into desulphoglucosinolates and a successive HPLC-UV quantitation, using desulphosinigrin as external standard and specific correction factors for each analyte. This method is based on indirect quantitation and accuracy is strictly related to the conversion yield. For a complete conversion, in fact, a reaction time of three days is required, so this kind of analysis is extremely long. Moreover UV detector is not very sensitive and selective and it could not provide an accurate quantification in less concentered samples. A direct, more robust and sensitive method could greatly optimize analysis time and could be applied into food industry for a quick and efficient quantification of these analytes into different matrices.

The aim of this work is the development and validation of an HPLC-ESI-MS/MS method for the simultaneous separation and quantification of intact glucosinolates and isothiocyanates. This method will be applied to different matrices containing glucosinolates, in order to trace their profile.

2.3 Experimental

2.3.1 Materials and reagents

Glucoraphanin (GRA) and glucoerucin (GER) as standards and rocket salad seeds, broccoli and crackers extracts were supplied by Consiglio per la Ricerca e la Sperimentazione in Agricoltura, Centro di Ricerca per le Colture Industriali of Bologna (CRA-CIN).

Sinigrin (SIN) standard was purchased from Sigma-Aldrich (Milano, Italy).

Sulforaphane (SFN) and erucin (ERN) standards were purchased from Santa Cruz Biotecnology (Texas, U.S.A).

2.3.2 Calibration standard

Glucoraphanin, glucoerucin and sinigrin standard stock solutions were prepared in water/methanol 50:50 (v/v) at a concentration of 5 mg/ml and stored at -20 °C. Standard working solutions were prepared by dilution of the stock solutions in water/methanol 50:50 (v/v), in order to obtain concentrations ranging from 5 to 500 µg/ml. These working solutions were stored at 4 °C and used at most for a week. Quality controls (QCs) at concentrations 1.7, 6.7 and 16.7 µg/ml were prepared before analysis by dilution of the working solutions in 5:95 (v/v) formic acid 0.5 % in acetonitrile/formic acid 0.5% in water.

Concerning isothiocyanates, sulforaphane and erucin stock solutions were prepared dissolving precise amounts of standard sample into acetonitrile, obtaining a final concentration of 2.5 mg/ml. These stock solutions were stored at -20 °C. Standard working solutions were prepared by dilution of stock solutions in acetonitrile, obtaining a final concentration in the range 5 – 250 µg/ml. These working solutions were stored at 4 °C at most for three days. Quality controls (QCs) at concentrations 16.7, 125 and 200 µg/ml were prepared before analysis by dilution of the working solutions in 5: 95 (v/v) formic acid 0.5 % in acetonitrile: formic acid 0.5% in water.

2.3.3 Liquid chromatography and mass spectrometry: method validation

Waters Alliance 2690 Chromatograph (Milford, MA, USA) with 120 positions autosampler and thermostat was used. Mass spectrometer triple quadrupole and electrospray interface (QUATTRO LC, Waters) was used for quali-quantitative analysis Analytical separation was conducted on a WATERS X-select CSHTM C18 5.0 µm (2.1 mm*150 mm) column

2.3.3.1 HPLC optimization

The mobile phase used to achieve a good separation between the main glucosinolates, glucoraphanin (GRA), sinigrin (SIN), glucoerucin (GER) and the main isothiocyanates, sulforaphane (SFR) and erucin (ER), was formic acid 0.5 % (v/v) in acetonitrile (solvent A) and formic acid 0.5 % (v/v) in water (solvent B) using a gradient elution (10 min at 5% A and 4 min at 24% A, 4 min at 50% A, 7 min at 80% A, 5 min at 5%) at 0.15 mL min^{-1} flow rate. The analytical column was maintained at 30°C and the sample volume injected was 20 µL. In the optimized analytical conditions, the mean retention times were for GRA 6.3± 0.2 min, SIN 8.2 ± 0.2 min, GER 16.9 ± 0.2 min, SFR 17.2± 0.1 min and ER 26.8 ± 0.2 min. The total ion chromatogram (TIC) for each analyte was reported in **Figure 23**.

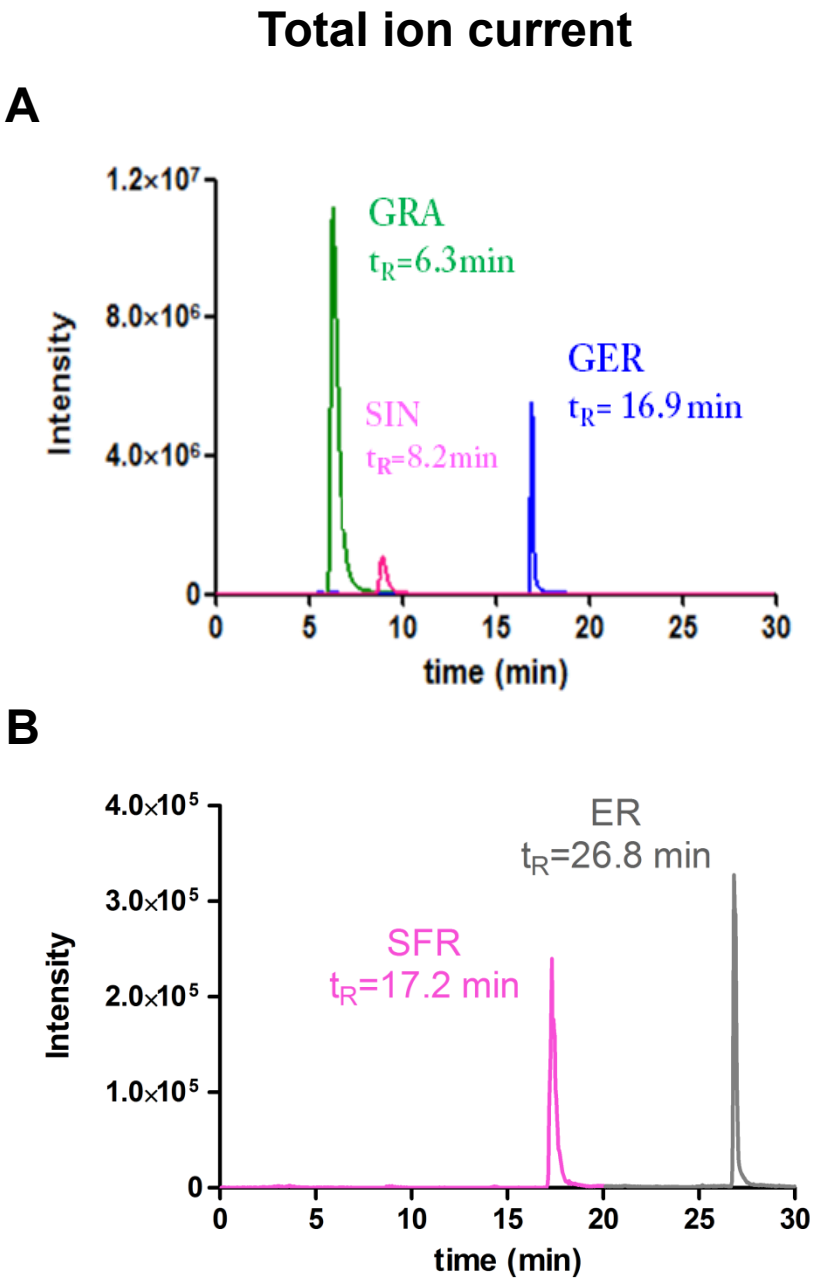

Figure 23. Total ionic current (TIC) of A) GLSs B) ITCs

2.3.3.2 ES mass spectrometry optimization

Ionization and revelation parameters were optimized for each analyte (**Table 6**).

Table 6. Ionization parameters for main Glucosinolates and isothiocyanates

Instrumental parameters	GRA	ER	SIN	SFR	ER
Ionization mode	-	-	-	+	+
Capillary voltage (kV)	3.0	3.0	3.0	3.0	3.0
Cone voltage (V)	35	35	35	15	15
Source temperature (°C)	130	130	130	130	130
Desolvation temperature (°C)	410	410	410	410	410
Nebulizer rate (L/h)	65	65	65	65	65
Desolvation rate (L/h)	1065	1065	1065	1065	1065
RCE (%) [a]	30	30	30		
Collision gas	Ar	Ar	Ar	Ar	Ar
Parent ion (*m/z*)	436	420	358	178	162
Daughter ion (*m/z*)	372	259	162	114	162

In **Figures 24-28** are reported MS/MS spectra for each analyte with respective fragmentation reactions.

For quantitation, each analyte molecular ion has been used, while for assessing specificity has been monitored the most intensive fragmentation reaction using MRM acquisition mode.

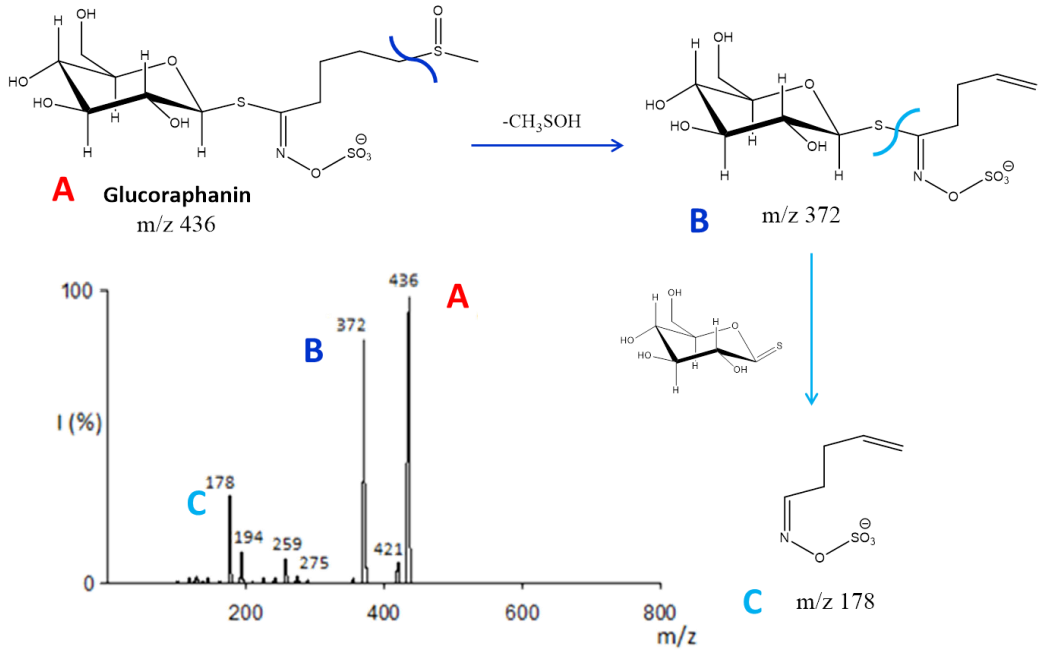

Figure 24. Glucoraphanin MS/MS spectrum

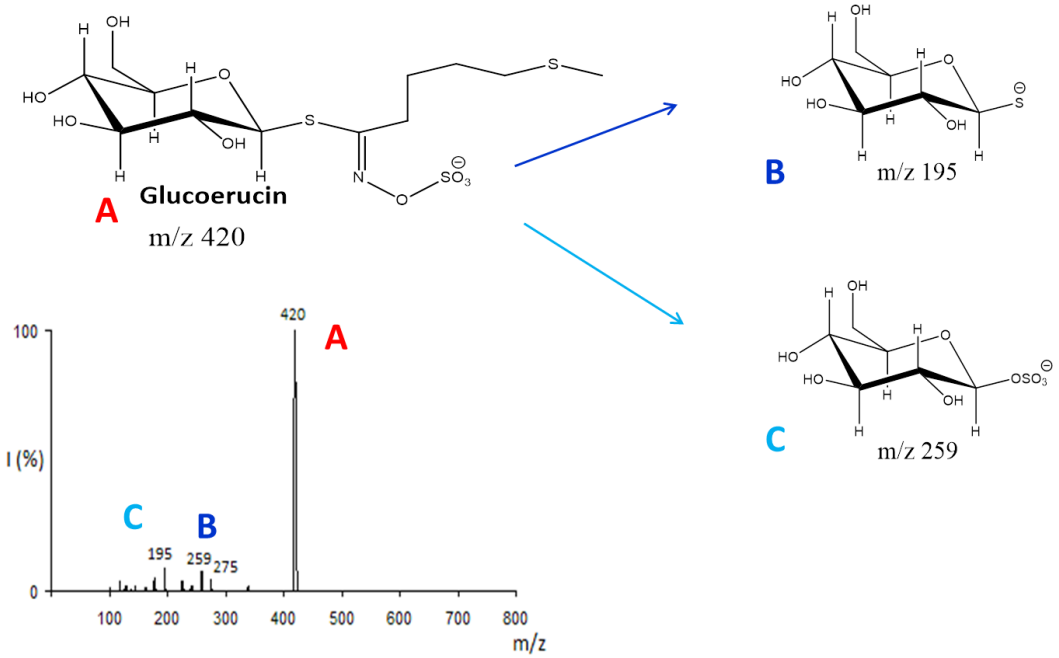

Figure 25. Glucoerucin MS/MS spectrum

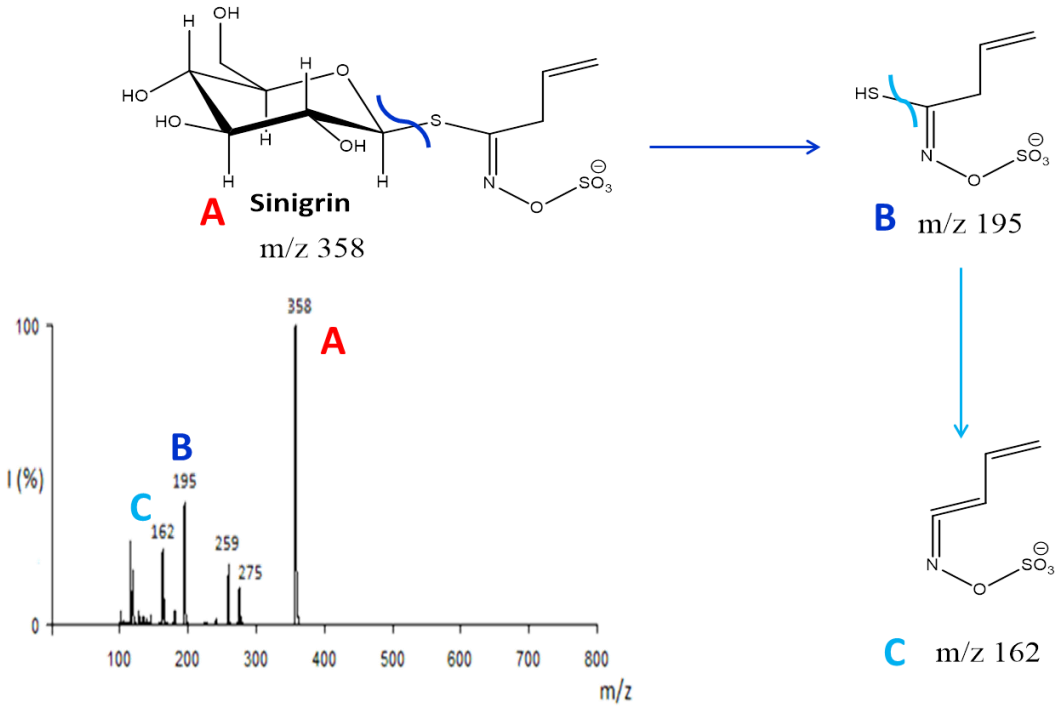

Figure 26. Sinigrin MS/MS spectrum

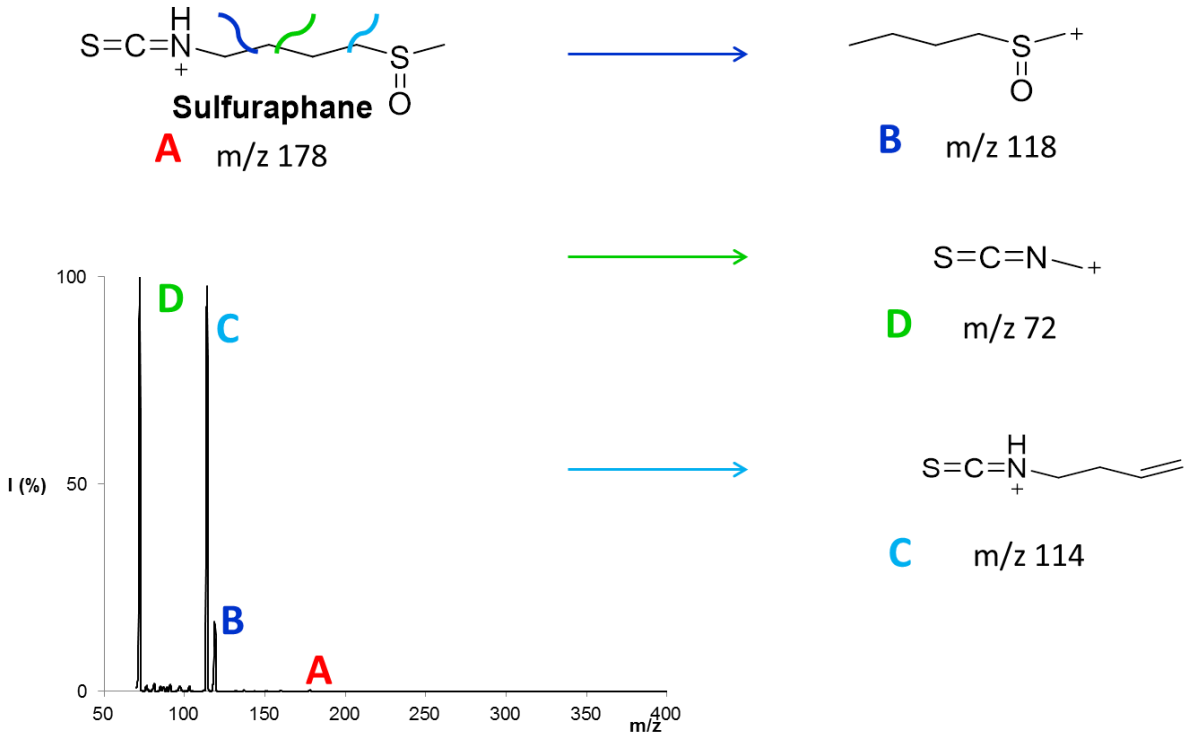

Figure 27. Sulforaphane MS/MS spectrum

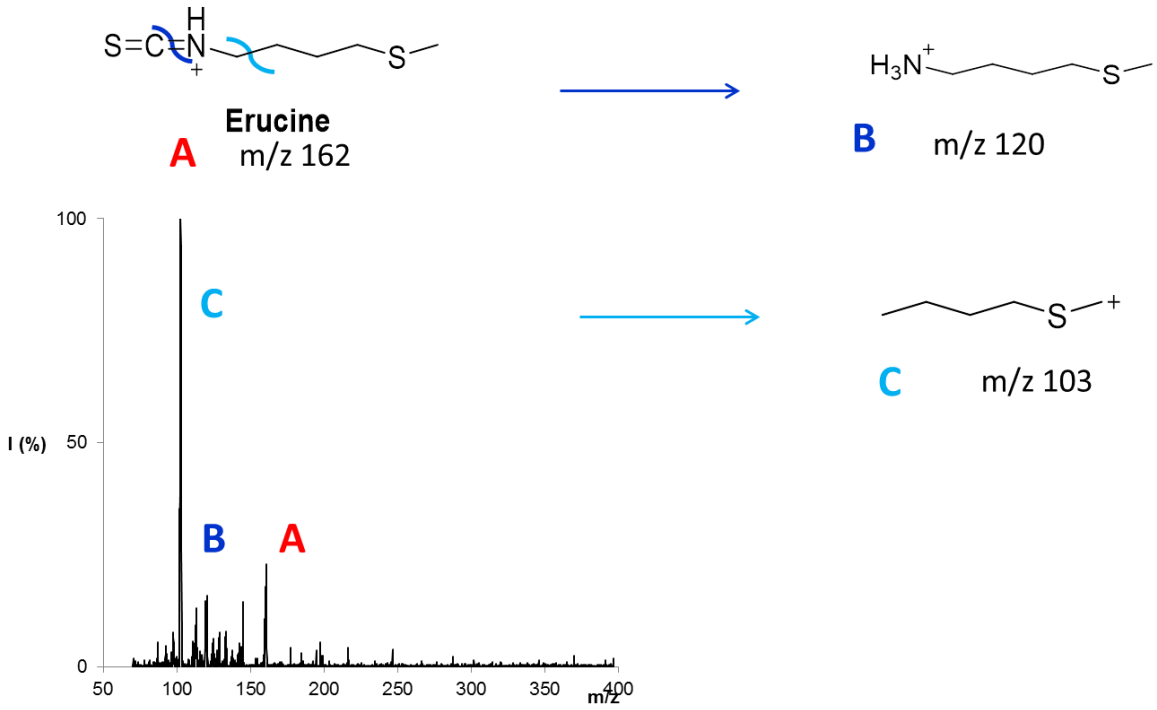

Figure 28. Erucin MS/MS spectrum

2.3.3.3 Method Validation

HPLC-ESI-MS/MS method has been validated according to ICH guidelines.

Detection limit (LOD) and quantitation limit (LOQ)

LOD and LOQ of each analyte, expressed as 3 and 10 times signal to noise ratio respectively, have reported in **Table 7**.

Table 7. LOD and LOQ values for glucosinolates and isothiocyanates

	LOD (ng/mL)	LOQ (ng/mL)
GRA	2.5	5.0
GER	5.0	25
SIN	25	100
SFR	50	100
ER	250	500

Linearity range

Linearity was studied in the range from 0.5 to 50 µg/ml for each glucosinolates and from 5 to 250 µg/ml for isothiocyanates.

Linear calibration curve parameters were obtained from the plot of the analyte peak area/internal standard peak area versus analyte concentration using a least squares regression analysis (weight = $1/x^2$). The performance of the analytical method was monitored using three quality control samples (QCs) having 4.5 nM for QC low, 20 nM for QC med and 45 nM for QC high.

Accuracy (bias %) and Precision (CV %)

Method precision and accuracy, expressed as bias% and CV% respectively, were determined intraday and interday using QCs samples. In **Table 8** and in are reported intraday and interday precision and accuracy values for glucosinolates and isothiocyanates.

Table 8. Precision and accuracy values for glucosinolates and isothiocyanates

	GRA		GER		SIN	
µg/mL	bias (%)	CV (%)	bias (%)	CV (%)	bias (%)	CV (%)
			Intraday			
1.67 (QC low)	0.92	-0.20	1.01	-9.78	0.38	-8.61
6.67 (QC med)	1.91	5.60	1.36	-10.0	1.18	-7.91
16.67 (QC high)	0.59	2.52	3.92	-1.99	1.32	1.86
			Interday			
1.67 (QC low)	2.91	1.60	1.86	-6.99	2.32	-2.20
6.67 (QC med)	1.67	8.70	2.06	-5.05	1.54	-1.40
16.67 (QC high)	0.91	4.58	0.58	6.50	1.35	6.68

Table 9. Precision and accuracy values for isothiocyanates

	SFR		ER	
µg/mL	bias (%)	CV (%)	bias (%)	CV (%)
		Intraday		
16.7 (QC low)	5.4	7.8	9.8	0.6
125 (QC med)	5.6	-6.6	4.8	-10.4
250 (QC high)	9.4	3.3	3.9	12.7
		Interday		
16.7 (QC low)	8.7	0.80	9.5	-8.8
125 (QC med)	3.0	-13.4	4.9	-7.9
250 (QC high)	3.8	12.6	1.9	8.5

2.3.4 Glucosinolates extraction procedures

The extraction of Broccoli, rocket salad and bakery products were performed in collaboration with CRA-CIN of Bologna.

Broccoli and rocket salad

300-500 mg of seeds or broccoli were ground to a fine powder, incubated in thermal bath at 90 °C for 10 minutes in 4 ml EtOH 70% and then sonicated for 30 minutes. Extracts obtained were centrifuged for 30 minutes at a speed of 39800 rpm at a temperature of +4 °C and then filtered. The remaining flour was washed with 4 ml EtOH on vortex for 1 minute and filtered.

Bakery product

The sample was incubated in a microwave system and analytes extracted setting 400 Watt as maximum power, heating gradient: 80 °C in 3 minutes and extraction at 80 °C for 10 minutes. Extracts were centrifuged at a speed of 25900 rpm at a temperature of +4 °C and filtered. The residue was retreated in microwave oven as described above,

the extract centrifuged, and filtered. These extracts were left for 48 hours at -20 °C, centrifuged for 30 minutes at 39800 rpm at +4 °C.

2.4 Results and discussion

2.4.1 Glucosinolates in rocket salad seeds

Rocket salad seeds extracts contain mainly glucoerucin and glucoraphanin, but in different amounts (

Figure 29). Two different kinds of seeds were analyzed: pressure disoiled seeds and hexane disoiled seeds. In particular, glucoraphanin amounts are about 0.5 µmol/g and 1.0 µmol/g, respectively, in pressure disoiled seeds and hexane disoiled seeds, while glucoerucin is about 90 µmol/g in both seeds. From these data arise that disoiling process influence the amount of glucoraphanin but not the amount of glucoerucin. Further analysis showed that a preliminary autoclaving process decrease the extraction yield of glucoerucin, but not of glucoraphanin, about of the 15%. Sinigrin concentration is under the LOD in all the samples analyzed.

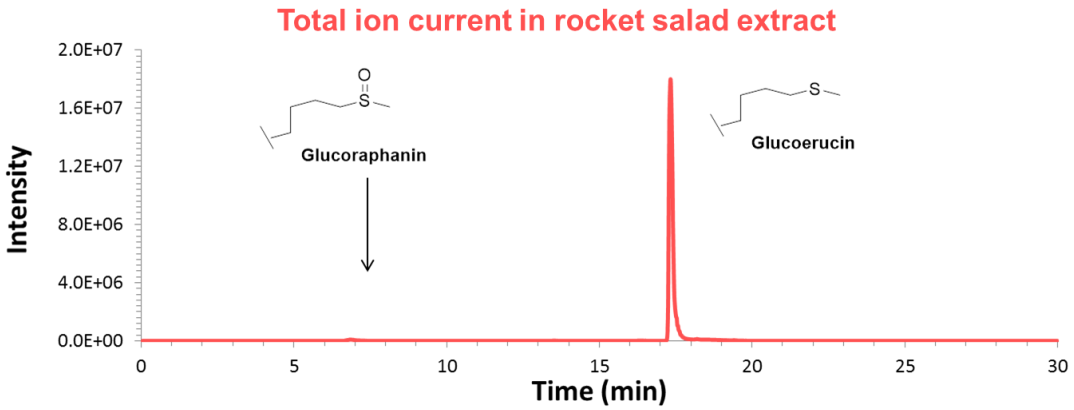

Figure 29. TIC of rocket salad seed extract

Before the analysis on samples, matrix effect (EM%) was evaluated for glucosinolates. For this purpose, samples spiked with known concentration of standard were analyzed and the recovery of the analyte was determined subtracting from the obtained value the endogen contribute. E.M.% values close to 100% show absence of matrix effect, higher and lower values than 100% indicate, respectively, ionic increase or ionic suppression.

Matrix effects (**Table 10**) are calculated as ratio of glucosinolate concentration in matrix and glucosinolate concentration in mobile phase.

Table 10. Matrix effect of GLSs in rocket seed

E.M. % ± DS in rocket seeds			
µg/ml	GRA	GER	SIN
1.67 (QC low)	104 ± 1.1	103 ± 4.3	104 ± 0.7
7.20 (QC med)	104 ± 1.7	101 ± 1.5	102 ± 1.5
16.7 (QC high)	101 ± 0.2	97 ± 1.5	100 ± 0.7

2.4.2 Glucosinolates in broccoli sprouts

Glucosinolates composition in broccoli is quite complex and very different from rocket seeds. Indeed, there are both aliphatic, as glucoiberin, epiprogoitrin, and aromatic glucosinolates, as glucobrassicin and neoglucobrassicin (**Figure 30**). These glucosinolates were not quantified, because their standards were not available. Concerning glucoraphanin, glucoerucin and sinigrin, their amount in broccoli extracts were 0.82, <LOD and 0.2 µmol/g respectively.

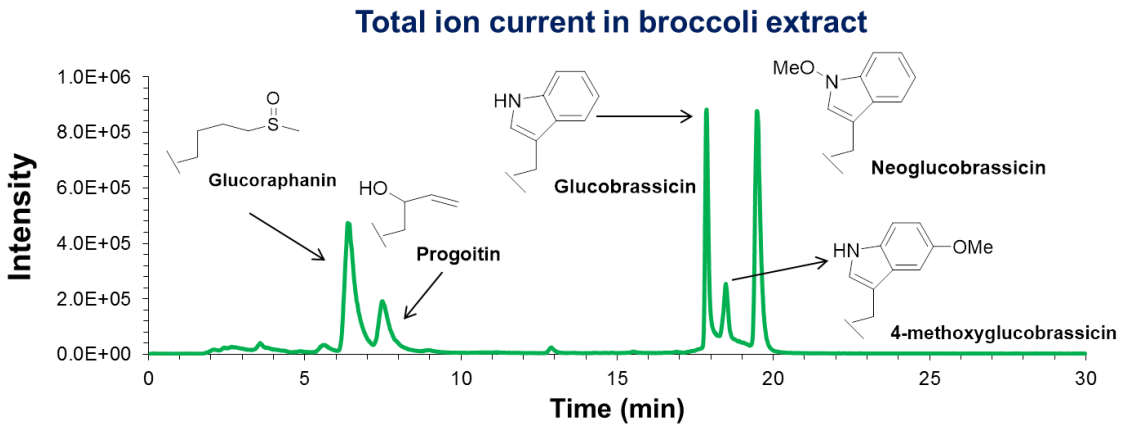

Figure 30. TIC of broccoli extract sample

Matrix effect in broccoli extract was evaluated for each analyte and results, expressed as %, are reported in Table 8. As reported, matrix effect in broccoli extract is negligible.

Table 11. Matrix effect of GLSs in broccoli extracts

E.M % ± DS in broccoli extracts			
µg/ml	GRA	GER	SIN
1.67 (QC low)	101 ± 2.7	108 ± 0.6	98.4 ± 1.4
7.20 (QC med)	103 ± 2.0	98 ± 2.9	102 ± 4.0
16.7 (QC high)	103 ± 1.9	99 ± 2.1	102 ± 1.8

2.4.3 Glucosinolates in bakery products

Bakery products extracts analyzed were obtained from two different flours. Specifically, in the first preparation was used a flour in which myrosinase is active, and one in which the myrosinase is deactivated.

In **Figure 31** was reported the total ion current of the two different bakery products. As observed, using the flour in which the myrosinase is active, the glucoerucin and

glucoraphanin amount was 0.1 µmol/g and <LOQ respectively. Unlike in the bakery product containing deactivated myrosinase flour the glucoerucin amounts was 10 times higher than that present in activated myrosinase flour (i.e. 1.2 µmol/g) and the amount glucoraphanin was 0.04 µmol/g.

Likely, during the fortification process and/or during the extraction GLSs could react with the myrosinase present in the flour, reducing their amount in the bakery product.

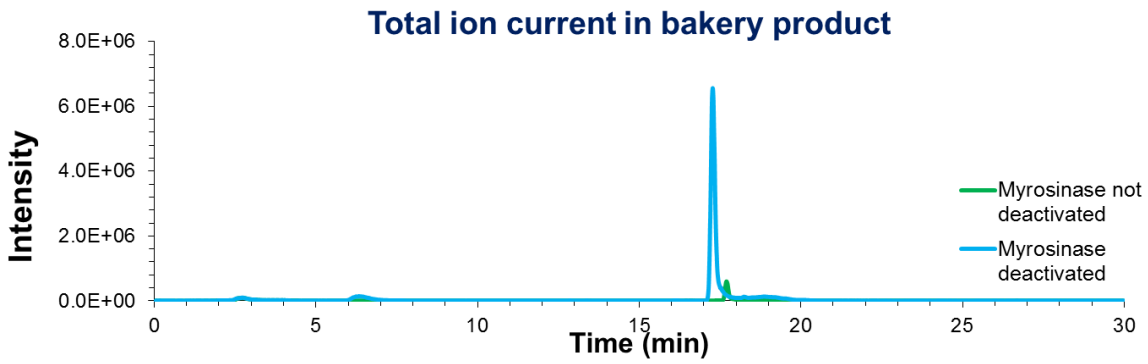

Figure 31. TIC of bakery product extract samples

2.5 Conclusions

An HPLC-ES-MS/MS method for the simultaneous determination of glucosinolates and isothiocyanates has been developed and optimized. This method has been validated according to ICH guidelines and is very sensitive and selective (GLSs LOQ< 100 ng/mL; ITCs <500ng/mL for each analytes), precise and accurate (bias % and CV% <10% for each analytes) and the matrix effect was less than 10% for each analytes.

This method is used to quantify the GLSs and ITCs present in rocket salad seeds, broccoli extract and also in bakery products.

The new developed method could replace the ISO 9167-1 method currently used based on an indirect quantitation of GLSs. Indeed, in the ISO method GLSs must be preliminary converted into desulphoglucosinolates, with reaction times up to three days and the risk of uncontrolled recovery of the derivative. Moreover the use of mass spectrometer in the developed method, in particular the MRM date acquisition mode, allow the elimination of many interferences in the matrix, increase sensitivity and selectivity and allow to separate partially co-eluting species acting also directly on the sample without any pre-analytical step.

This method could greatly optimize analysis time and could be applied into food industry for a quick and efficient quantification of these analytes into different matrices.

Chapter 3

Drugs co-administration: OCA and bile acid sequestrants

Drug-drug interactions could results in different systemic exposure, causing variations in the activity of co-administered drugs. The simultaneous administration of two drugs could be synergistic (when the drug's effect is increased) or antagonistic (when the drug's effect is decreased) or a new effect can be produced. However, interactions may also exist between drugs and foods, as well as drugs and medicinal plants or herbs.

The drug-drug interaction may also increase the risk of side effects. On the other hand, if the action of a drug is reduced it may break off the therapeutic effect because of under dosage.

Therefore, the preliminary evaluation of potential drug interactions is important before the market approval as well as during the post-marketing period.

3.1.1 Obeticholic acid: pharmacological activity, metabolism and physicochemical properties

Obeticholic acid (OCA, **Figure 32**) is a semi-synthetic analogue of the primary bile acid (BA) chenodeoxycholic acid (CDCA), which is a natural ligand of the nuclear hormone receptor farnesoid X receptor (FXR).

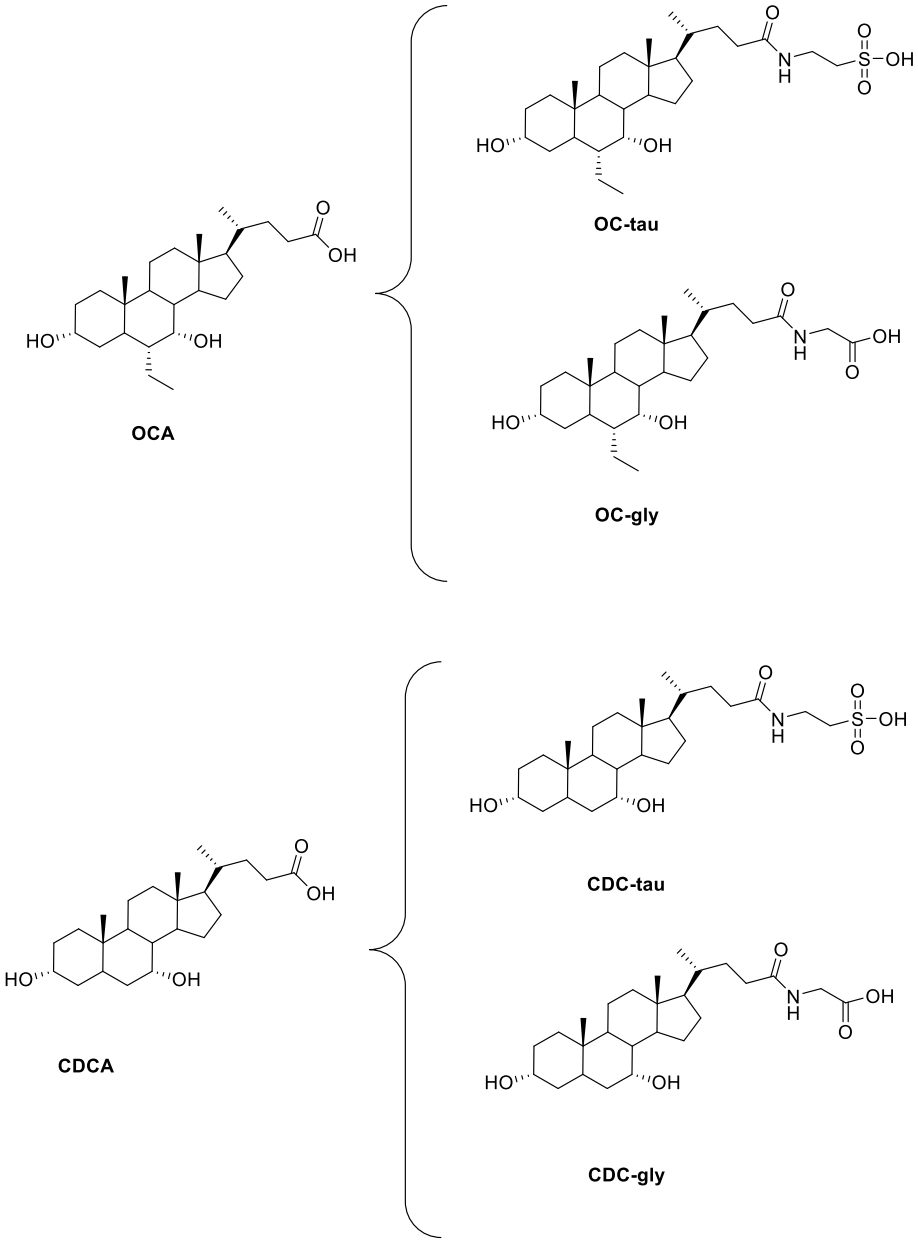

Figure 32. Chemical structures of OCA and CDCA and their taurine and glycine conjugates

FXR constitutes a negative feedback regulator in the hepatic synthesis of BAs from cholesterol through the repression of cholesterol 7α- hydroxylase (CYP7A1). This step is a limiting step of the entire biosynthesis, conjugation and transport of BAs. Activation of FXR inhibits BA synthesis and protects against the toxic accumulation of BAs.

OCA is undergoing development in phase 2 and 3 studies for specific liver and gastrointestinal disorders, as primary biliary cirrhosis (PBC).

PBC is an autoimmune liver disease, in which the destruction of the bile ducts that transport bile acids out of the liver, resulting in cholestasis, was observed.

If untreated, or if a patient does not adequately respond to treatment, chronic inflammation and fibrosis can advance to cirrhosis liver failure, and death.

There is no known cure for PBC but previous studies suggested that treatment with FXR agonists should be beneficial. The agonist potency (EC50) of OCA was 100 times higher than its endogenous analogue (0.15 vs 15 μM)[44].

The metabolism of OCA is quite similar to CDCA (**Figure 32**)**.** Indeed, study in vivo reports that OCA was mainly metabolized in glycine (OC-gly) and taurine (OC-tau).

Concerning the physicochemical properties of OCA, they are quite similar to CDCA, including solubility, lipophilicity and critical micellar concentration (**Table 12**) as well as their metabolites.

Table 12. Physicochemical properties of OCA, CDCA and their metabolites

	CDCA	**CDC-gly**	**CDC-tau**	**OCA**	**OC-gly**	**OC-tau**
Solubility (μM)	32	7	h.s.	9	1.3	h.s.
CMC (mM)	3.2	2.0	3.0	2.9	1.7	1.8
LogP$_{A-}$	2.2	0.4	0.9	2.5	0.6	1.0

h.s. high solubility

3.1.2 Bile acids sequestrants: cholestyramine and colesevelam

The bile acid sequestrants (called also resins) are polymeric compounds used in the treatment of chronic diarrhea due to bile acid malabsorption and/or in the therapy of pruritus associated with cholestasis. Indeed, bile acid sequestrants bind BA) in the gastrointestinal tract modifying their enterohepatic circulation and preventing their re-absorption from the gut. In addition to BAs, bile acid sequestrants could also bind drugs in the GI tract, preventing their absorption into the bloodstream. For this reason, it is generally advised that they could be spaced several hours apart from other drugs.

The main bile acid sequestrants on the market are cholestyramine and colesevelam (**Figure 33**), active pharmaceutical ingredients of Winthrop and Welchol respectively. The interaction of these resins with BA (sequestrant) increases the conversion of Cholesterol to BA as a negative feedback mechanism resulting also in a reduction of cholesterol in the body.

Cholestyramine is a strong ion exchange resin, in which its chloride anions exchange with anionic bile acids in the gastrointestinal tract and bind them strongly in the resin matrix. Its anion functional group is a quaternary ammonium group attached to an inert styrene-divinylbenzene copolymer.

Colesevelam hydrochloride is made by crosslinking polyallylamine with epichlorohydrin, and then modifying it with bromodecane and (6-bromohexyl) trimethylammonium bromide. The bromide ions are then replaced with chloride ions when the material is washed[45].

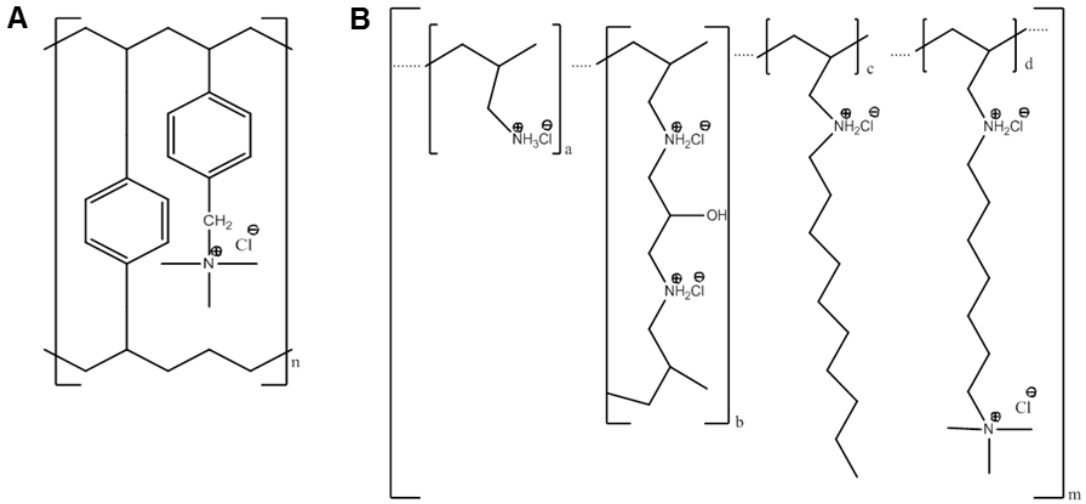

Figure 33. Structure of A) Cholestyramine B)Colesevelam

3.1.3 Adsorption isotherms

Adsorption isotherm describes the equilibrium of the sorption of a compound at a surface when the temperature is constant. It represents the amount of material bound (q_e) at the surface as a function of the material present in solution. The most frequently used isotherms[46] are the linear isotherm, Freundlich isotherm, and the Langmuir isotherm.

Linear isotherm

Formally the linear adsorption isotherm resembles Henry's law. The linear isotherm (**Equation 1**) can be used to describe the initial part of many practical isotherms. In this case, the amount of analytes absorbed at equilibrium (q_e) is proportional to the concentration of analyte unabsorbed in solution at equilibrium (C_{eq}) in the solution at equilibrium with a the distribution coefficient (K_d).

$$q_e = K_d \cdot C_{eq}$$

Equation 1. Linear isotherm

Freundlich isotherm

Freundlich isotherm is commonly used to describe the adsorption for the heterogeneous surface based on the empirical equation (**Equation 2**).

$$q_e = K_F \cdot {C_{eq}}^{1/n}$$

Equation 2. Freundlich isotherm

The constant K_F is an approximate indicator of adsorption capacity, while 1/n is a function of the strength of adsorption in the adsorption process.

If n=1 then the partition between the two phases are independent of the concentration and this expression reduces to a linear adsorption isotherm. If value of 1/n is below one it indicates a normal adsorption while when 1/n is above one it indicates cooperative adsorption. The function has an asymptotic maximum as pressure increases without bound.

Langmuir isotherm

The Langmuir isotherm describes quantitatively the formation of a monolayer adsorbate on the adsorbent surface between solid and liquid phases.

The model assumes that 1) all of the adsorption sites are equivalent and each site can only accommodate one molecule; 2) the surface is energetically homogeneous and the adsorbate-adsorbate interaction is considered negligible compared to the interactions of adsorbate-adsorbent; 3) there are no phase transitions. Based upon these assumptions, Langmuir represented in **Equation 3.**

$$q_e = \frac{q_m \, b \, C_{eq}}{1 + b \, C_{eq}}$$

Equation 3. Langmuir isotherm

Where qm is the maximum adsorption capacity and b the affinity of sorbent for the analytes.

3.2 Aim and rationale

In the treatment of PBC, a new semisynthetic bile acid, the obeticolic acid (OCA) has been developed. PBC is a liver disease that primarily results from autoimmune destruction of the bile ducts that transport bile acids (BAs) out of the liver, resulting in cholestasis. Previous studies suggested that treatment with FXR agonists should be beneficial in cholestatic diseases as PBC. Among them, OCA has shown agonist potency (EC50) more 100 times higher than that of its endogenous analogue CDCA[44]. A common symptom of PBC is itch caused by BAs in circulation which would normally be removed by the liver.

To relieve itching, a bile acid sequestrant, as cholestyramine and colesevelam, are prescribed to absorb BAs in the gut and be eliminated.

During the development of a new drug, the interaction drug-to-drug had to be investigated especially when two or more drugs are used in combination to treat a disease or condition, as required by FDA.

Regarding the treatment of PBC, the therapeutic effect of OCA could be reduced by a co-administration of BAs sequestrant. Indeed, OCA could be adsorbed by BAs sequestrant and not only the endogenous bile acids.

For this reason, the aim of this work is the development of an in vitro model for the determination and quantification of the interactions between OCA and colesevelam and cholestyramine in terms of maximal binding capacity (q_m) and affinity adsorbent (b) to the OCA and its main metabolites.

3.3 Experimental

3.3.1 Materials and reagents

Cholestyramine was purchased from Sigma Aldrich, and Colesevelam was a kind gift of Daiichi Sankyo (courtesy of Dr. Ken Jones). OCA and its glycine and taurine N-acylamidates (conjugates) were provided by the Department of Pharmaceutical Science, University of Perugia, Italy. CDCA and its glycine and taurine conjugates and BES (N,N-Bis(2-hydroxyethyl)-2-aminoethanesulfonic acid) were purchased from Sigma Aldrich.

3.3.2 HPLC-ES-MS/MS method

Bile acid concentration was determined by HPLC-ES-MS/MS in the following experimental conditions:

HPLC column: Phenyl-hexyl column (XSelect) 4μm, 150 x 2.1 mm

Mobile phase composition and elution mode: Solvents A is a 15 mM ammonium acetate buffer (pH = 8.00) and Solvent B was acetonitrile: methanol = 75:25 v/v

Time (min)	A%	B%	Flow (ml/min)	Curve
0	65	35	0.15	1
10	65	35	0.15	1
10.3	55	45	0.15	6
21	55	45	0.15	1
21.3	0	100	0.15	6
23.3	0	100	0.15	1
24	65	35	0.15	6
35	65	35	0.15	1

The HPLC was connected to an Quattro-LC (Micromass) MS system operating in the negative ion mode with a MRM acquisition method with the following parameters:

Instrumental parameters	Value		
Capillary	3.0 KVolts		
Cone			
OCA	70		
OC-gly	60		
OC-tau	85		
Extractor	8 volts		
RF lens	0.07 volts		
Source block temp.	130ºC		
Desolvation temp.	200ºC		
MS			MS2
Entrance	1.0 volts	Entrance:	0.0 volts
Exit	1.0 volts	Exit:	1.0 volts
Ion energy	1.5 volts	Ion energy:	3.0 volts
LM resolution	12	LM resolution:	12
HM resolution	12	HM resolution:	12
Pressure			
Analyser vacuum	$4.2e^{-5}$ mBar		
Gas cell	$2.4e^{-3}$ mBar		
Flows			
Nebulizer (Nitrogen)	87 lit/hr		
Desolvation gas (Nitrogen)	800 lit/hr		
Multiplier	650 volts		

For OCA the transition m/z 419.5 $\rightarrow$ 419.5 was monitored (no fragmentation product ions were observed). For the glycine conjugate of OCA (OC-gly) the transition m/z 476.2 $\rightarrow$ 73.8 was monitored. This fragment is typical of the loss of the glycine moiety. For OC-tau the transition m/z 526.2 $\rightarrow$ 79.9 was monitored. This fragment is typical of the loss of the taurine moiety.

The used method has been validated and fulfilled all the standard criteria of accuracy, precision; the LOQ was adequate to evaluate the concentration of the different BA in the analyzed solutions[44].

3.3.3 Adsorption experiments of bile acids by bile acid sequestrants

Since one of the assumptions of the Langmuir isotherm provides that the adsorbate-adsorbate interaction is considered negligible compared to adsorbate-adsorbent interactions, it was decided to work in a range of concentrations below the critical micellar concentration (CMC) to avoid that the binding with the resin might be hindered by the micelles formation.

BA sorption experiments were carried out in BES (N,N-Bis(2-hydroxyethyl)-2-aminoethanesulfonic acid) 0.05M pH=7.2. BES is a zwitterionic buffer that has no affinity for bile acid sequestrants. The dry BA sorbent (0.003g), *i.e*. cholestyramine or and colesevelam, was suspended in the buffer solution (V, 3mL) with a given initial concentration of BA (C0), covering the range of 0.3-1.5mM. The mixture was rigorously stirred for 24h at 37°C. Then the suspension was centrifuged, appropriately diluted and analyzed.

The amount of BA bound was calculated as the difference between the total amount of bile acids introduced into the system and the amount of unabsorbed bile acid. The maximum binding capacity of each sequestrant was calculated according to the Langmuir isotherm equation:

$$q_e = \frac{q_m \, b \, C_{eq}}{1 + b \, C_{eq}}$$

where:

Qe	amount of BA absorbed at equilibrium (mmol/g)
Qm	maximum adsorption capacity (mmol/g)

B	affinity of sorbent for BA (mM^{-1})
Ceq	concentration of unabsorbed BA in solution at equilibrium (mM)

The values of qm and b were determinated by plotting 1/qe versus 1/ Ceq:

$$\frac{1}{q_e} = \frac{1}{q_m b}\frac{1}{C_{eq}} + \frac{1}{q_m}$$

3.4 Results and discussion

3.4.1 Adsorption experiments of bile acids by bile acid sequestrants

Cholestyramine

The adsorption isotherms for the binding of OCA and CDCA and its glycine and taurine conjugates to cholestyramine are shown in **Figures 34-36**. The maximum adsorption capacity (qm) for OCA, OC-tau and OC-gly was very similar to that of the corresponding endogenous bile acids (Table1) while their affinity for of cholestyramine was greater than those of the endogenous bile acids (CDCA, CDC-gly, and CDC-tau).

Indeed, the affinity of cholestyramine for OCA was 5.3 times greater than CDCA, for OC-gly was 1.5 times greater than CDC-gly and for OC-tau was 2.0 times greater than for CDC-tau.

It has been demonstrated that the forces involved in bile salt anion-cholestyramine interaction are primarily of electrostatic nature but are reinforced by an additional nonelectrostatic interaction of the hydrophobic face of the steroid nucleus of bile acids with the hydrophobic portion of the resin; the strength of the latter force is dependent on the degree of hydrophobicity of the adsorbate molecule. Therefore, the additional 6α-ethyl group in OCA, and its conjugates is the likely explanation for its greater affinity for the sequestrants.

In a previous study we measured the 1-cotanol/water partition coefficient $LogP_{o/w}$ of OCA, and observed that is was greater than that of CDCA -- 2.5 vs 2.2 -- further supporting the involvement of nonelectrostatic interactions.

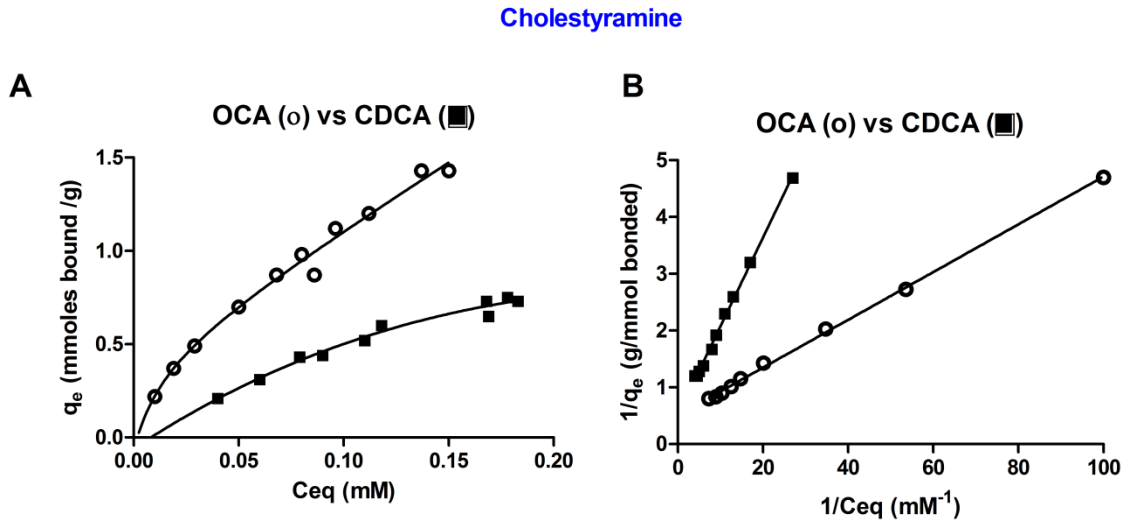

Figure 34. A) Adsorption isotherms for binding of OCA (o) and CDCA (■) to cholestyramine B) Langmuir isotherms for the adsorption of OCA (o) and CDCA (■) to cholestyramine

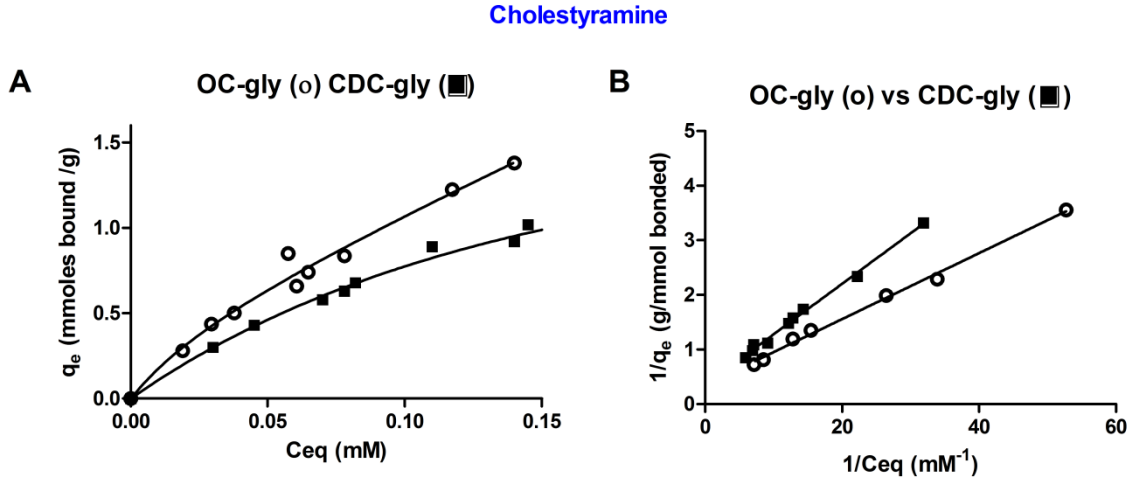

Figure 35. Adsorption isotherms for binding of OC-gly (o) and CDC-gly (■) to cholestyramine B) Langmuir isotherms for the adsorption of OC-gly (o) and CDC-gly (■) to cholestyramine

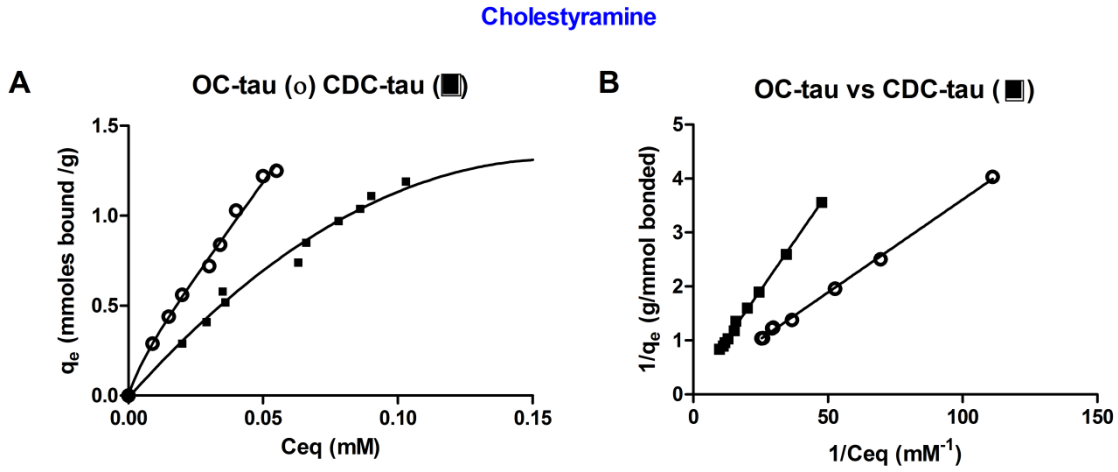

Figure 36. A) Adsorption isotherms for binding of OC-tau (○) and CDC-tau (■) to cholestyramine B) Langmuir isotherms for the adsorption of OC-tau (○) and CDC-tau (■) to cholestyramine

Table 13. Coefficients of adsorption isotherms obtained for cholestyramine

Cholestyramine	CDCA	OCA	CDC-gly	OC-gly	CDC-tau	OC-tau
Slope	0.17	0.050	0.093	0.060	0.057	0.029
Intercept	0.398	0.393	0.353	0.349	0.321	0.321
qm (mmol/g)	2.5	2.5	2.8	2.9	3.1	3.1
b (mM-1)	2.3	12.3	3.8	5.8	5.6	11.2

The comparison between the adsorption isotherms for the binding of OCA, OC-tau and OC-gly to cholestyramine was reported in **Figure 37**. The maximum capacity for OCA, OC-gly and OC-tau was very similar, while the affinity of cholestyramine for OCA was greater than its taurine and glycine conjugates, respectively 1.1 times and 2.1 times.

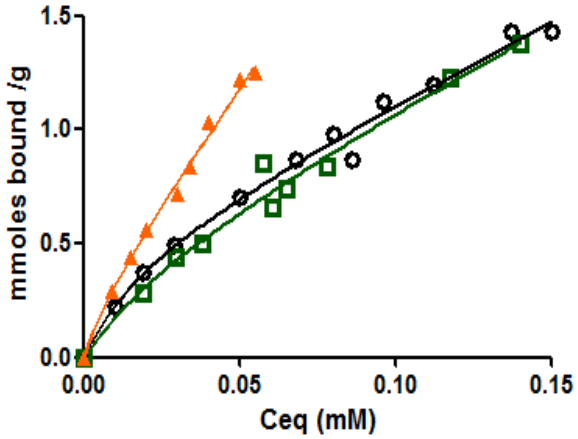

Figure 37. Adsorption isotherms for binding of OCA (○), OC-gly (□) and OC-tau (▲) to cholestyramine

Colesevelam

The adsorption isotherm for the binding of OCA and CDCA and its glycine and taurine conjugates to colesevelam were reported in **Figure 38-40**. The maximum adsorption capacity (qm) for OCA, OC-tau and OC-gly is was very similar to respective endogenous bile acids (Table2) while their affinity of colesevelam was greater than that of CDCA. Indeed, the affinity of colesevelam for OCA is 2.8 times greater than CDCA, for OC-gly is 1.9 times greater than CDC-gly and for OC-tau is 1.5 times than CDC-tau.

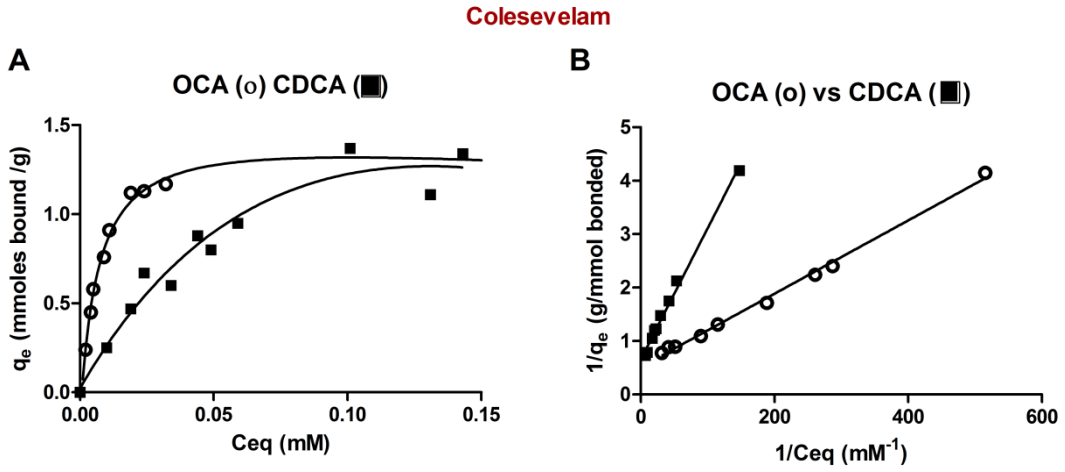

Figure 38. A) Adsorption isotherms for binding of OCA (○) and CDCA (■) to colesevelam B) Langmuir isotherms for the adsorption of OCA (○) and CDCA (■) to cholestyramine

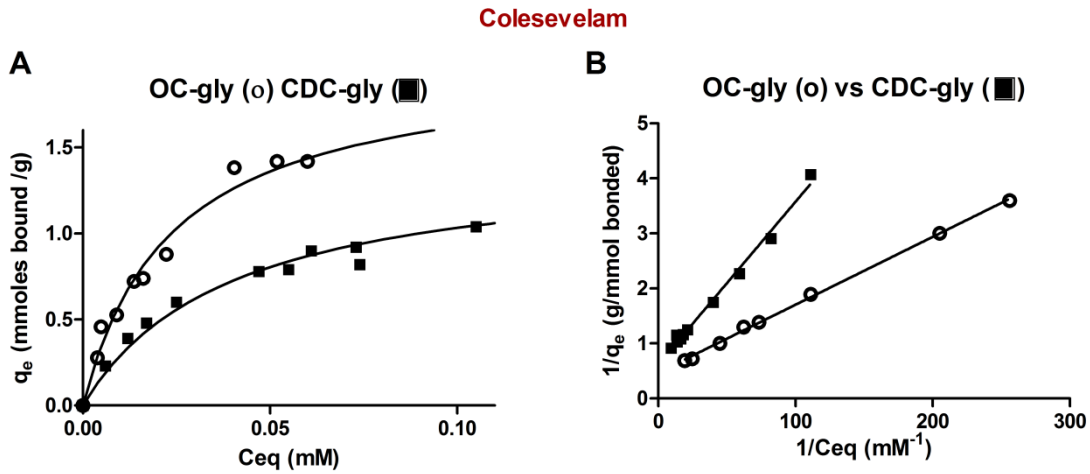

Figure 39. A) Adsorption isotherms for binding of OC-gly (○) and CDC-gly (■) to colesevelam B) Langmuir isotherms for the adsorption of OC-gly (○) and CDC-gly (■) to colesevelam

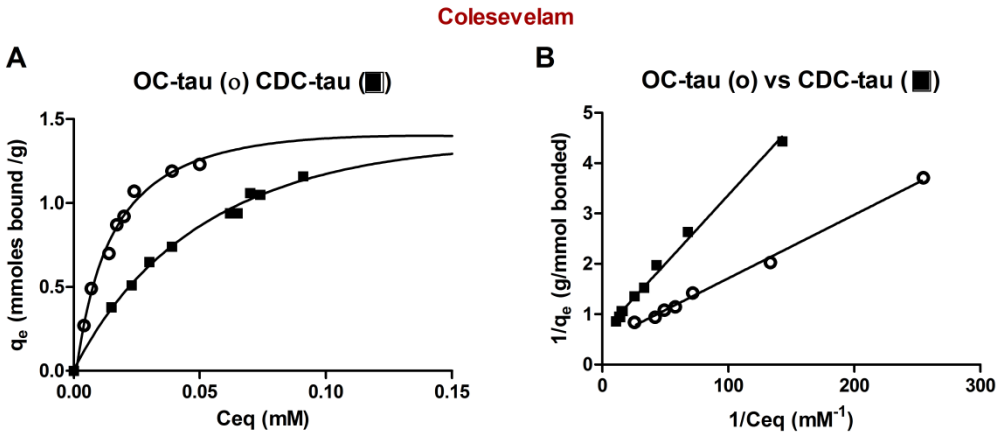

Figure 40. A) Adsorption isotherms for binding of OC-tau (○) and CDC-tau (■) to colesevelam B) Langmuir isotherms for the adsorption of OC-tau (○) and CDC-tau (■) to colesevelam

Table 14. Coefficients of adsorption isotherms obtained for colesevelam

Colsevelam	CDCA	OCA	CDC-gly	OC-gly	CDC-tau	OC-tau
Slope	0.024	0.007	0.030	0.0123	0.027	0.0126
Intercept	0.657	0.535	0.610	0.471	0.636	0.4513
qm (mmol/g)	1.5	1.9	1.6	2.1	1.9	2.1
b (mM-1)	27.4	76.3	20.3	38.3	23.5	35.8

The adsorption isotherms for the binding of OCA, OC-tau and OC-gly to colesevelam are shown in **Figure 41**. The affinity of colesevelam for OCA was greater than those of its taurine and glycine conjugates, respectively 2.1 times and 2.0 times while the maximum capacity was very similar.

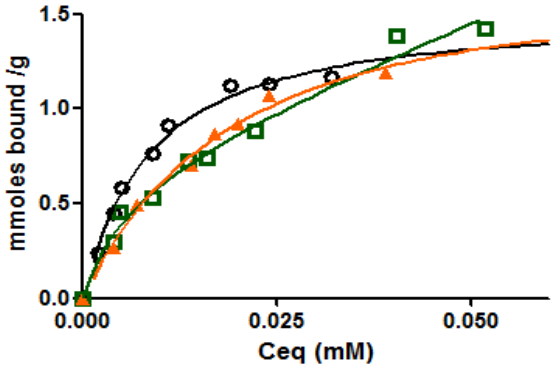

Figure 41. Adsorption isotherms for binding of OCA (○), OC-gly (□) and OC-tau (▲) to colesevelam

3.4.2 Comparison between colesevelam and cholestyramine adsorption

The adsorption isotherms for the binding to colesevelam of OCA and CDCA and its glycine and taurine conjugates compared with cholestyramine were reported in **Figure 42**. The maximum capacity of OCA, OC-tau and OC-gly was slightly greater for cholestyramine than colesevelam while the affinity of bile acids for colesevelam was much greater than that of cholestyramine 6.2 times for OCA, 6.6 times for OC-gly and 3.2 times for OC-tau.

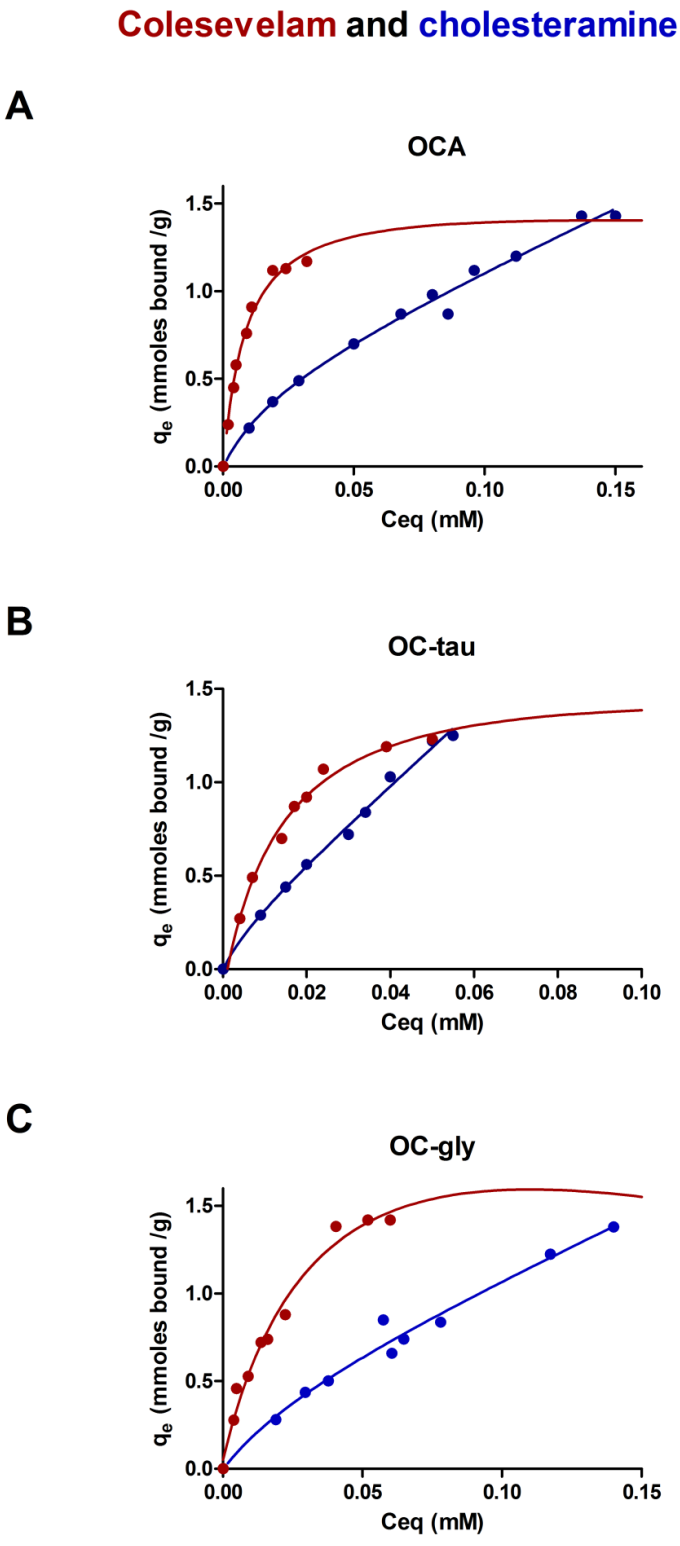

Figure 42. Comparison of the adsorption isotherms of OCA to cholestyramine (blu) and colesevelam (red)

3.5 Conclusions

The results of these adsorption experiments indicate that OCA, OC-tau and OC-gly exhibited greater binding to the bile acid sequestrants, colesevelam and cholestyramine, than their corresponding endogenous bile acids CDCA, CDC-tau and CDC-gly. The implication of these findings is that dosing of bile acid sequestrants at the same time as that of OCA is likely to decrease the intestinal absorption of OCA. In addition, the sequestrants will also bind the glycine and taurine conjugates of OCA and therefore active also under steady-state chronic regiments.

In conclusion the co-treatment of OCA and the bile acid sequestrant must be avoided in order to maintain the appropriate level of OCA in the enterohepatic circulation. The co-treatment is also no recommended by administering the two drugs at different time since the sequestrant are able to bind efficiently also the active metabolites of OCA i.e. OC-gly and OC-tau.

Chapter 4

Electron ionization in LC-MS:

Direct-EI-UPLC-MS for sterols analysis

Nowadays, commercially available liquid chromatography-mass spectrometry (LC-MS) interfaces are based on atmospheric pressure ionization techniques (API). Among them, electrospray (ESI) and atmospheric pressure chemical ionization (APCI) are the most common ionization sources.

Nevertheless, these soft ionization sources show few, critical restraints[47,48]. Firstly, the signal response of ESI and APCI is strongly influenced by the polarity and ionization properties of the analytes. ESI and APCI, indeed, are suitable for compounds characterized by a medium-high polarity while less polar molecules request a chemical derivatization before the analysis to introduce functional group prone to ionization. Secondly, the structural information obtained with these sources could be insufficient especially for unknown substances since the quasi-intact molecular ion is produced. Therefore, the coupling with tandem MS (MS-MS) or MS^n is required to obtain more information on structure by further ionize and fragment the ion. However, there are not MSMS electronic libraries to match the mass spectra obtained. Furthermore, the quantitative analysis in ESI and APCI is often influenced by matrix effects causing an under or over-estimation.

The solution of these problems could be the LC and electron ionization-mass spectrometry (EI-MS) coupling[47,48]. Indeed, EI is not influenced by the polarity of the analyte and its mass spectra represent a real chemical fingerprint for each molecule. Fragments, molecular-ion abundance and their biodistribution in the EI mass spectrum are unique, highly reproducible and collected in electronic libraries (NIRST, National Institute of Standard and Technology).

Unfortunately, LC and EI-MS seem to be incompatible "unfriendly" analytical techniques. Indeed, EI operates in high-vacuum and the presence of liquid effluent could make it instable, decreasing the instrument performance. The solvent elimination represents the main obstacle in the LC-EI-MS coupling because it should be performed without influencing the sample ionization. The first device that combine EI and HPLC was developed in 1984 by Willoughby and Browner and it based on a particle beam (PB) interface in which the solvent was eliminated through a gas-phase momentum separation. Despite initial success of PB interface, this interface was quickly abandoned because of its scarce sensitivity, signal instability and limited linearity especially in reverse phase. The coupling between LC and EI-MS was forgotten for ages but recently two different approaches, supersonic molecular beam (SMB) and Direct-EI interface, was proposed.

4.1 Direct-EI interface[47,48]

Direct-EI interface was designed and totally realized in Italy at University of Urbino and nowadays it is commercially available combined with nano-LC systems.

The name "Direct-EI" was chosen to emphasize the direct connection between the LC-column and EI ion source without intermediate apparatus. Indeed, in the Direct-EI interface, fused silica capillary tubing connects the separation system with EI source passing from an atmospheric pressure region to high vacuum. In this way the transition between liquid to gas phase is carried out inside the EI.

The interface mechanism is based on an aerosol formation in high-vacuum condition followed by a quick droplet desolvation and analyte vaporization. Once the transition from liquid to gas phase is completed, the mix of vapors homogeneously distributed inside source block are exposed to the "impact" of the electron beam (**Figure 43**).

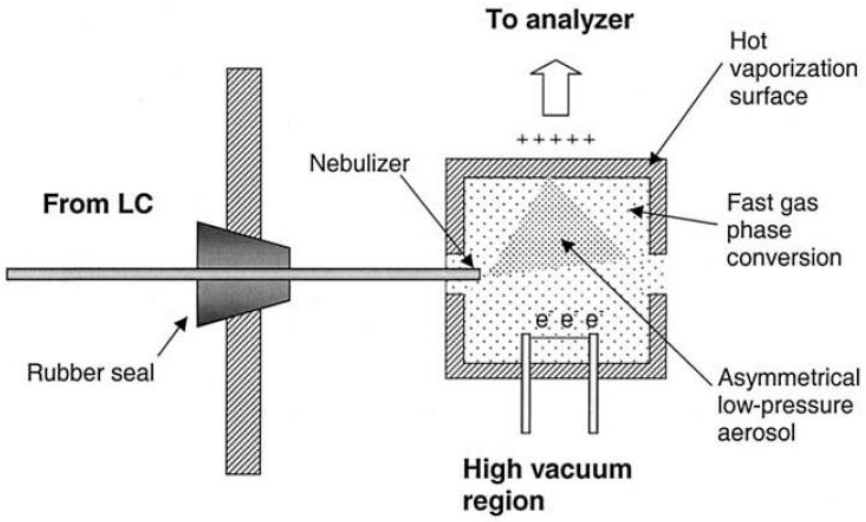

Figure 43. Direct-EI interface

The temperature of the ion source was usually settled between 300 and 400°C to compensate for the latent heat of vaporization during the droplet desolvation and to convert the solute into the gas phase.

The separation module coupled with Direct-EI should operate at nano-scale flow rate (100-500 nL/min) without exceeding the 750 nL/min, in order to obtain the best analytic performance. This strict dependence on nano-flow represents the main restraint in the use of Direct-EI LC-MS interface. Indeed, the most nano-LC systems are less widespread in a analysis laboratory than HPLC or UHPLC. The new challenge in the research focused on Direct-EI is its coupling with UHPLC systems operating at higher flow rate (200-500 µL/min) without significant performance decreases. Several splitting devices are currently tested to optimize the best split ratio[49].

4.2 Aim and rational

Steroids are a big family of small molecules with a wide polarity range starting from neutral liphofilic sterols including cholesterol and its close metabolites or intermediate, steroid hormones and acidic ionized steroid such as bile acids. One of the main challenges in steroids analysis is develop high sensitivity LC-MS methods without derivatization and mobile phase additives. These pretreatments are often necessary because compounds less polar as steroids could be not efficiently ionized by soft ionization source conventional coupled with LC-MS system.

The use of Direct-EI-LC-MS in steroids analysis of can offer several advantages in comparison with current GC and HPLC-MS method: i) the sample preparation procedures can be carried out without derivatization; ii) the signal response is not influenced by the polarity of the analytes and not affected by matrix effect; iii) a more complete structural information can be obtained from EI-MS spectrum due to the high fragmentation and the comparison with electronic library.

This work represents a feasibility studied focused on the optimization of Direct-EI-UHPLC-MS methods for the determination of impurity profiling of 17β-estradiol (**Figure 44**) steroids analysis and the simultaneous determination of nonalcoholic steatohepatitis (NASH) biochemical markers[50] as cholesterol, desmosterol and lathosterol (**Figure 45**).

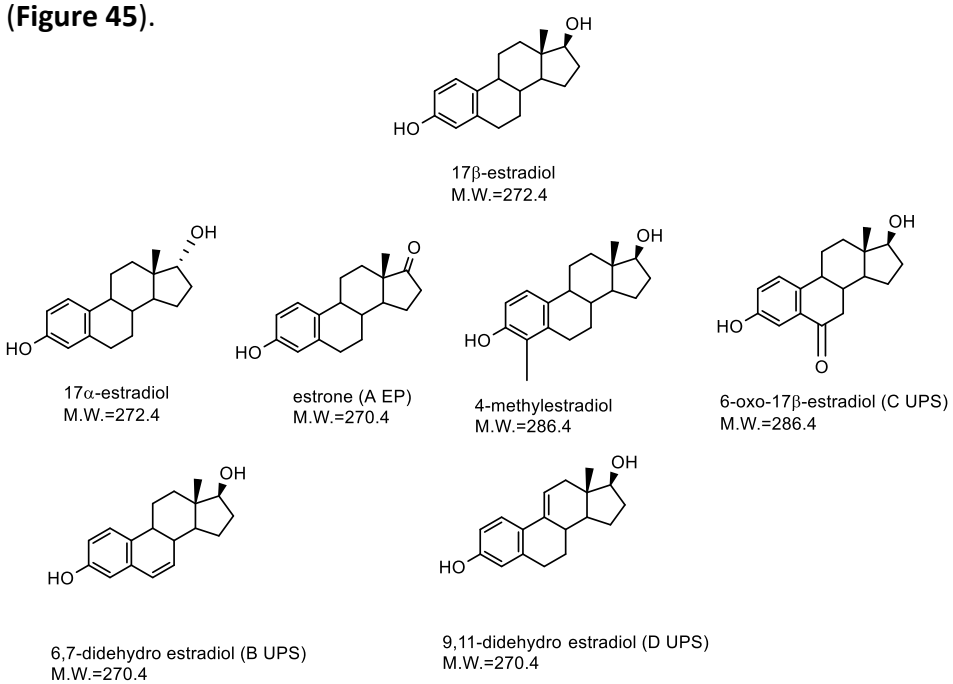

Figure 44. Chemical structures of 17β-estradiol and its impurities

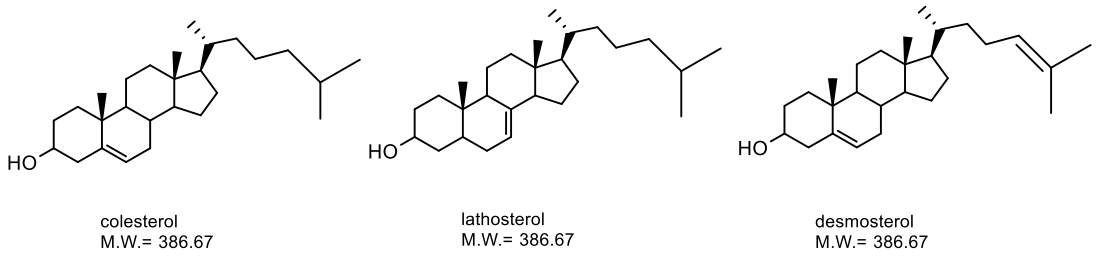

Figure 45. Nonalcholic Steatopepatitis biomarker

4.3 Preliminary data

Direct-EI-UHPLC-MS method

Liquid chromatography was carried out with an Agilent 1290 Infinity UHPLC system. A splitting device allowed to adapt the UHPLC flow rate (200-500 µL/min) using a 1:500 ratio. An Agilent 7000A QQQ mass detector was equipped with a Direct-EI interface. The splitting device was placed at the interface entrance and right after the injector. All standards were injected individually in flow injection analysis (50:50 v:v H_2O:ACN) to record their mass spectra. Injection volumes spanning from 2 to 10 µL were delivered with autosampler. Scan experiments were performed from m/z 80 to 600, 2.4 cycles/sec. The ion source temperature was set at 350°C.

Standard solutions of 17β-estradiol and its impurities (6-oxo-17β-estradiol; 17α-estradiol; 6,7-didehydroestradiol; 9,11-didehydroestradiol; estrone; 4-methylestradiol) and for nonalcoholic steatohepatitis biomarkers (cholesterol, lathosterol and desmosterol) were prepared in ethanol at 50 µg/mL and directly injected to verify signal response and to record their EI-MS spectra.

Preliminary data and future perspective

EI-MS experimental spectra obtained for 17β-estradiol, 17α-estradiol, estrone, cholesterol, lathosterol and desmosterol are compared with NIRST EI-MS spectra, showing a matching >70% while the EI-MS spectra of the other 17β-estradiol impurities are not present in electronic library.

Regarding the determination of 17β-estradiol purity by HPLC-ES-MS or HPLC-UV, in previous studies 6,7 and 9,11-didehydroestradiol chromatographic separation is not reached[51]. Since their EI-MS spectra (**Figure 46**) are significantly different using direct-EI-LC-MS, they could be accurately quantified as well as for lathosterol and cholesterol (**Figure 47**).

In conclusion, the results demonstrated that Direct-LC-EI-MS can be successfully applied for sterol analysis showing several advantages.

In particular, the coupling of direct-EI- MS and LC may provide legally defensible, reproducible and easy-to interpret mass spectra for the unambiguous identification during impurity profiling of 17β-estradiol in pharmaceutical preparation with no matrix effects.

The development and validation of Direct-EI-UHPLC-MS methods are currently carried out both for 17β-estradiol and its impurities. This method will be applied to the determination of 17β-estradiol purity in pharmaceutical tablet and its chemical stability after stress tests in which its degradation products will be identified and characterized.

Concerning NASH biomarkers, their quali-quantitative composition in plasma may be simultaneously evaluated avoiding derivatization and matrix effect thus facilitate the clinical utility of this analysis.

Direct-EI-UHPLC-MS allows to reduce significantly the analysis time and the amount of plasma sample required, thus stimulating its use in bioanalitical chemistry.

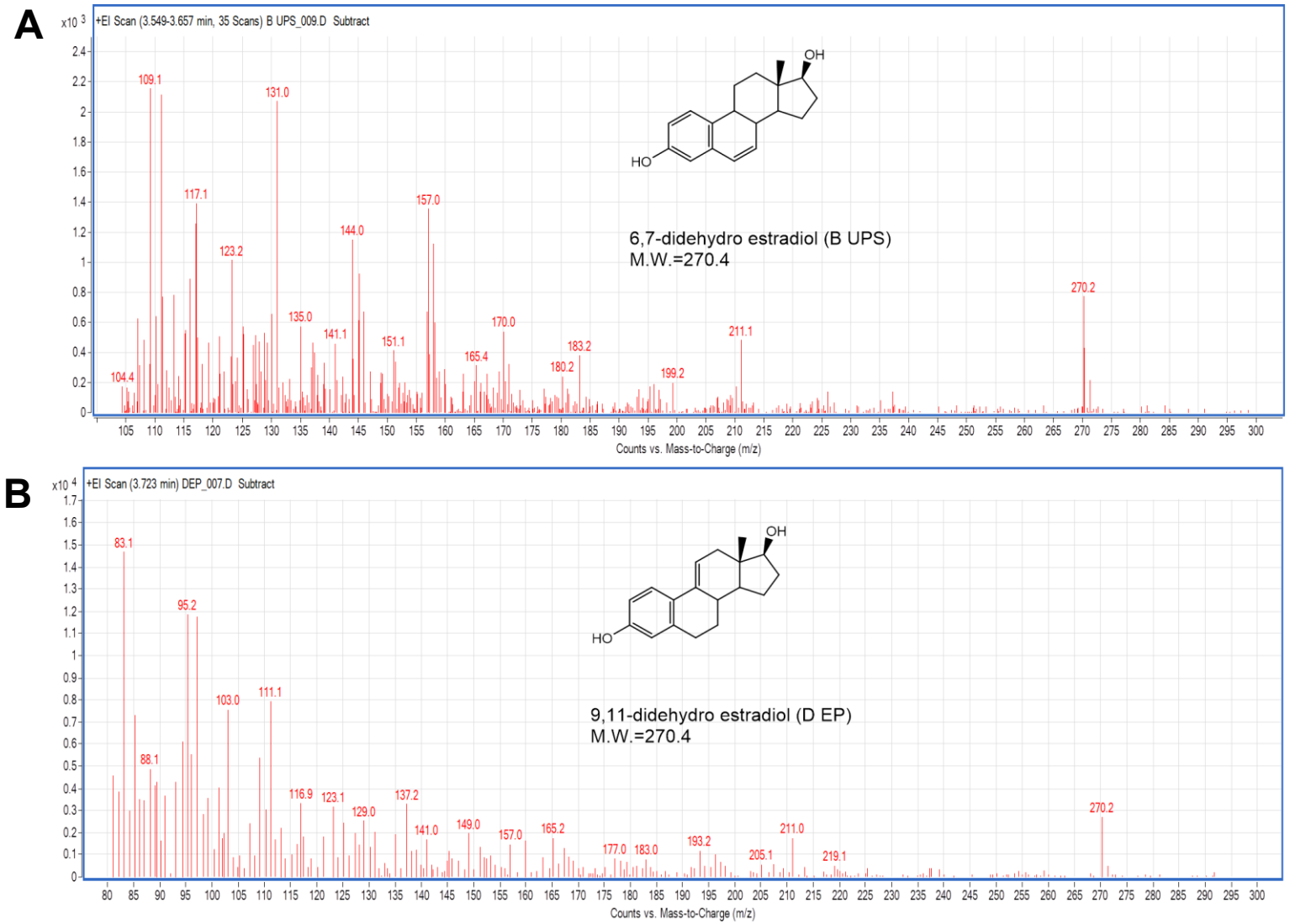

Figure 46. EI-MS spectra of A)6,7-didheydroesradiol B) 6,7-didheydroesradiol

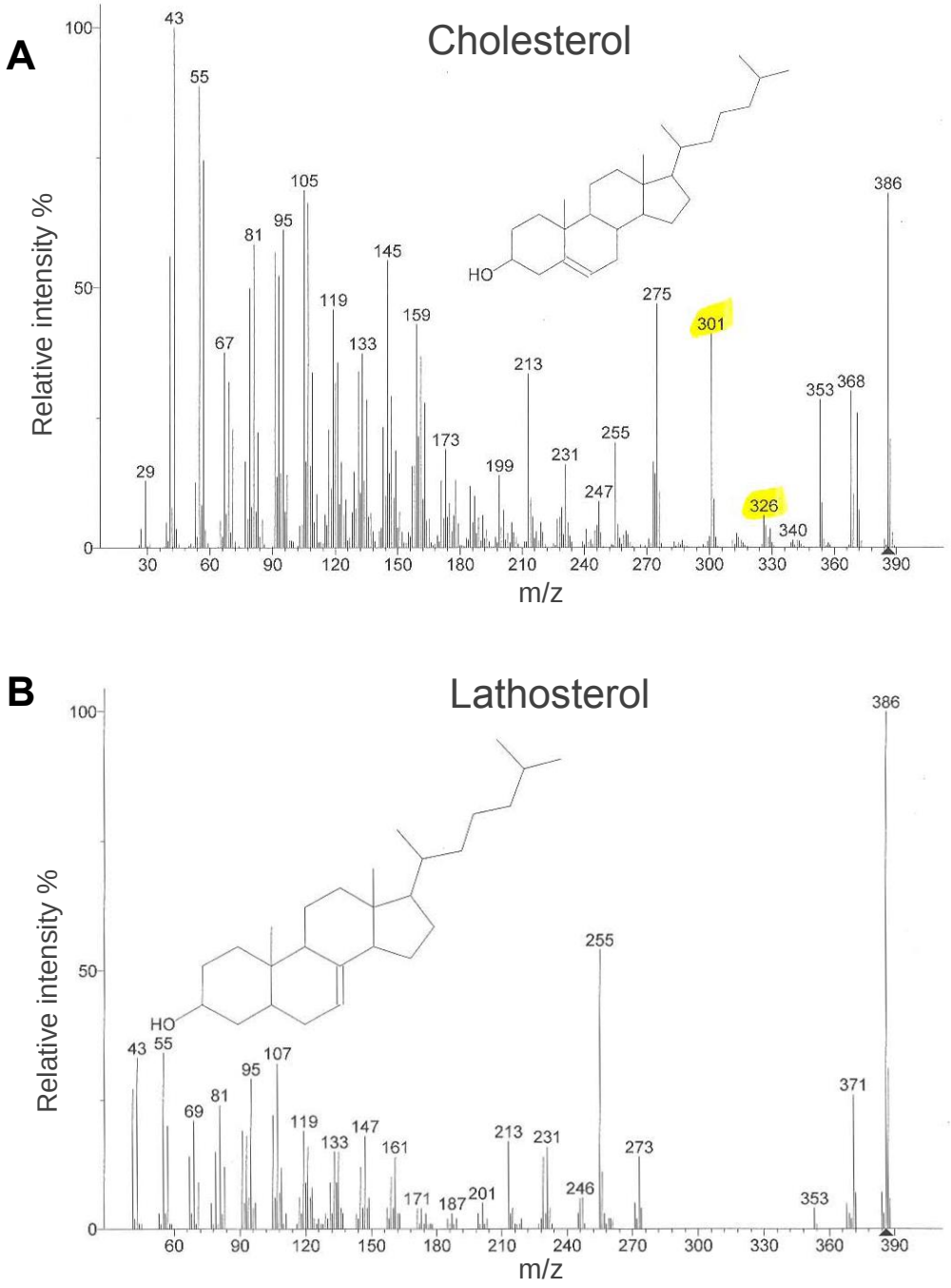

Figure 47. EI-MS spectra of A) cholesterol B) lathosterol

References

1) Keservani, R.K.; Kesharwani, R.K.; Vyas, N.; Jain, S.;Raghuvanshi,R.; Sharma, A.K. Der Pharmacia Lettre, 2010, 2 (1), 106-116

2) Bentley, K. W. Nat. Prod. Rep. 1997, 14, 387-411

3) Sarma, B. K.; Pandey, V. B.; Mishra, G. D.; Singh, U. P. Folia Microbiol. 1999, 44, 164-166.

4) Kuo, C. L.; Chi, C. W.; Liu, T. Y. Cancer Lett. 2004, 203, 127-137.

5) Iwasa, K.; Kim, H. S.; Wataja, Y.; Lee, D. U. Eur. J. Med. Chem. 1998, 33, 65-69.

6) Gudima, S. O.; Memelova, L. V.; Borodulin, V. B.; Pokholok, D. K.; Mednikov, B. M.; Tolkachev, O. N.; Kochetkov, S. N. Mol. Biol. (Moskow) 1994, 28, 1308-1314

7) Ni, Y. X. Zhong Xi Yi Jie He Za Zhi 1988, 8, 711-713, 707

8) Kim, T. S.; Kang, B. Y.; Cho, D.; Kim, S. H. Immunology 2003, 109, 407-414

9) Ikekawa, T.; Ikeda, Y. J. Pharmacobiodyn. 1982, 5, 469-474

10) Kong, W.; Wei, J.; Abidi, P.; Lin, M.; Inaba, S.; Li, C.; Wang, Y.; Wang, Z.; Si, S.; Pan, H.

11) Li, Y.; Ren, G.; Wang, Y. X.; Kong, W. J.; Yang, P.; Wang, Y. M.; Li, Y. H.; Yi, H.; Li, Z. R.; Song D. Q.; Jiang, J. D.J. Transl. Med. 2011, 9: 62, 1-10

12) Y-H Li, Bioorg Med. Chem., 2010, 18, 6422-6428

13) Li, Y. H.; Li, Y.; Yang, P.; Kong, W. J.; You, X. F.; Ren, G.; Deng, H. B.; Wang, Y. M

14) Das, B.; Srinivas, V. N. S. Synth. Commun. 2002, 32, 3027-3029

15) Food and Drug Administration. Guidance for Industry: Bioanalytical Method

16) Hu, Y. J.; Liu, Y.; Xiao, X. H. Biomacromolecules 2009, 10, 517−521.

17) Hu, Y.; Ehli, E. A.; Kittelsrud, J.; Ronan, P. J.; Munger, K.; Downey, T.; Bohlen, K.; Callahan, L.; Munson, V.; Jahnke, M.; Marshall, L. L.; Nelson, K.; Huizenga, P.; Hansen, R.; Soundy, T. J.; Davies, G. E. Phytomedicine 2012, 19, 861−867.

18) Spinozzi, S.; Colliva, C.; Camborata,C.; Roberti, M.; Ianni, C.; Neri,F.; Calvarese, C.; Lisotti, A.; Mazzella,G.; Roda, A. J. Nat. Prod. 2014, 77, 766−772

19) Jeon, Y. W. Bull. Korean Chem. Soc., 2002, 23, 391-394

20) Sun Ahe, K. Biochemistry 1998, 37, 16316-16324

21) Jin-Jian Lu, Wei Pan, Yuan-Jia Hu*, Yi-Tao Wang*, PLoS ONE, 2012, 7

22) Moreno, D.A.; Carvajal, M.; L´opez-Berenguer C.; Garc´ıa-Viguera, C. J. Pharm. Biomed. Anal., 2006, 41, 1508–1522

23) Bennett, R.N.; Mellon F.A.; Botting N.P.; Eagles J.; Rosa E.A.S.; Carvalho R. J. Agric. Food Chem. 2007, 55, 67-74

24) Underhill E.W., Wetter L.R., Chisholm, M.D. Biochem. Society Symp. 1973; 38: 303-326.

25) Zareba G, Serradelf N. Drug Future. 2004; 29: 1097–1104.

26) Kjñr A, Conti J. Acta Chemica Scandinavica. 1954; 8: 295-298

27) Delaquis P.J, Mazza G. Food Technology. 1995; 49: 73-79
28) Mayton, H.S.; Olivier C.; Vaughn, S.F.; Loria, R. Phytopathology.1996; 86,267-271
29) Wallig, M.A.; Belyea, R.L.; Tumbleson, M.E. Anim. Feed Sci. Technol. 2002 99, 205–214.
30) Schone, F.; Winnefeld, K.; Kirchner, E.; Grun, M.; Ludke, H.; Hennig, A. Anim. Feed Sci. Technol. 1990, 30, 143–154.
31) Burel, C.; Boujard, T.; Escaffre, A.M.; Kaushik, S.J.; Boeuf, G.; Mol, K.A.; Van der Geyten, S.; Kuhn, E.R. Brit. J. Nutr. 2000c. 83, 653–664
32) Tripathi, M.K., Mishra, A.S., Misra, A.K., Mondal, D., Karim, S.A. Small Rumin. Res.2001c, 39, 261–267.
33) Zang, X.P.; Tanii, H.; Kobayashi, K.; Higashi, T.; Oka, R.; Koshino, Y.; Saijoh, K. Arch. Toxicol. 1999, 73, 22–32
34) Tanii, H.; Takayasu, T.; Higashi, T.; Leng, S.; Saojoh, K. Food Chem. Toxicol. 2004, 42, 453–458.
35) Ahlin, K.A.; Emmanuelson, M.; Wiktorsson, H. Acta Vet. Scand. 1994, 35, 37–53.
36) Fenwick, G. R., Griffiths, N.M.; Heaney, R.K.J Sci Food Agric.1982, 34, 73-80.
37)Njumbe Ediagea, E.; Di Mavungua, J. D.; Scippob, M.L.; Schneiderc, Y.J.; Larondellec, Y.; Callebautd, A.; Robbense, J.; Van Peteghema,C.; De Saegera, S.; J. Chromatography A, 2011, 1218, 4395– 4405
38) Christensen, B.W.; Kjaer, A.; Olsen, C.E.; Olsen, O.; Sorensen, H. Tetrahedon, 1982, vol. 38; 353-357
39) Ares, A.; Nozal, M.; Bernal, J.L.; Bernal, J. Food Chemistry, 2014, Vol. 152, 66-74.
40) Bell, L.; Wagstaff, C. J. Agric. Food Chem. 2014, 62, 4481−4492
41) Kim, D. J.; Han, B. S.; Ahn, B.; Hasegawa, R.; Shirai, T.; Ito, N.; Tsuda, H. Carcinogenesis 1997, 18, 377−381
42) Tripathi, M. K.; Mishra, A. S. Anim. Feed Sci. Technol. 2007, 132, 1−27
43) Verkerk, R.; Schreiner, M.; Krumbein, A.; Ciska, E.; Holst, B.; Rowland, I.; De Schrijver, R.; Hansen, M.; Gerhauser, C.; Mithen, R.; Dekker, M. Mol. Nutr. Food Res. 2009, 53, S219−S265
44) Roda, A.; Pellicciari, R.; Gioiello, A.; Neri, F.; Camborata, C.; Passeri, D.; De Franco, F.; Spinozzi, S.; Colliva, C.; Adorini, L.; Montagnani, M.; Aldini, R.; J Pharmacol Exp Ther. 2014. 350(1),56-68
45) US Patent 5,607,669
46) Dada, A.O.; Olalekan, A.P.; Olatunya, A.M. J. App. Chem. 2012, 3, 38-45
47) Cappiello, A.; Famiglini,G.; Palma,P; Pierini,E.; Termopoli,V; Trufelli,H. Mass Spect Rev.2011.30, 1242– 1255
48) Palma, P.; Famiglini, G.; Trufelli, H.; Pierini, E.; Termopoli, V.; Cappiello, A. Anal Bioanal Chem. 2011, 399, 2683–2693

49) Cappiello, A.; Famiglini, G.; Mangani, F.; Palma, P.; Siviero A. Anal Chim Acta. 2003, 125–136
50) Simonen, M.; Mannisto, V.; Leppanen, J.; et all. , Hepatol. 2013, 58(3),976-982
51) Schulz, K.; Oberdieck, U.; Witschies, W. Pharmazie. 2013. 68, 311–316